Stem Cell Reports
Article

OPEN ACCESS

Defining Differences among Perivascular Cells Derived from Human Pluripotent Stem Cells

Maureen Wanjare,[1,4] Sravanti Kusuma,[1,2,4] and Sharon Gerecht[1,3,*]
[1]Department of Chemical and Biomolecular Engineering, Johns Hopkins Physical Sciences-Oncology Center and Institute for NanoBioTechnology
[2]Department of Biomedical Engineering
[3]Department of Materials Science and Engineering
Johns Hopkins University, 3400 N. Charles Street, Baltimore, MD 21218, USA
[4]These authors contributed equally to this work
*Correspondence: gerecht@jhu.edu
http://dx.doi.org/10.1016/j.stemcr.2014.03.004

SUMMARY

Distinguishing between perivascular cell types remains a hurdle in vascular biology due to overlapping marker expressions and similar functionalities. Clarifying and defining heterogeneities in vitro among perivascular cells could lead to improved cell-based tissue regeneration strategies and a better understanding of human developmental processes. We studied contractile vascular smooth muscle cells (vSMCs), synthetic vSMCs, and pericytes derived from a common human pluripotent stem cell source. Using in vitro cultures, we show unique cell morphology, subcellular organelle organization (namely endoplasmic reticulum, mitochondria, and stress fibers), and expression of smooth muscle myosin heavy chain and elastin for each cell type. While differences in extracellular matrix deposition and remodeling were less pronounced, the multipotency, in vivo, migratory, invasion, and contractile functionalities are distinctive for each cell type. Overall, we define a repertoire of functional phenotypes in vitro specific for each of the human perivascular cell types, enabling their study and use in basic and translational research.

INTRODUCTION

The vasculature is a multicellular system in which each cell type plays an important and indispensible role in its function. The inner lining of endothelial cells (ECs), which are in direct contact with the blood, is surrounded and supported by perivascular cells—either vascular smooth muscle cells (vSMCs) or pericytes. vSMCs surround larger vessels such as arteries and veins, whereas pericytes typically surround smaller microvessels and capillaries (Alberts et al., 2002). The disparate vessel locations for each perivascular cell type suggest that further differences exist that should be investigated and better understood in vitro in order to appropriately rebuild blood vessels for therapeutic applications (Dar and Itskovitz-Eldor, 2013; Wanjare et al., 2013b).

As the vasculature's support system, perivascular cells are primarily responsible for imparting contractility and producing and depositing extracellular matrix (ECM) proteins. Both cell types migrate to sites of angiogenesis, the growth of blood vessels from preexisting ones, to help stabilize and mature nascent endothelial tubes. Whether pericytes and vSMCs function similarly in these regards and to what extent have been unclear.

Along with the aforementioned functional similarities, perivascular cell types also exhibit overlapping marker expression. Adding to this complexity, neither perivascular cell type can be distinguished by one marker alone; instead, a combination of markers is needed for their identification. For example, both cell types have been demonstrated to express alpha smooth muscle actin (α-SMA). The expression of α-SMA and the transmembrane chondroitin sulfate proteoglycan neuron-glial 2 (NG2) help distinguish pericytes in different vessel types (Crisan et al., 2012); pericytes of the capillaries are $NG2^{+}\alpha\text{-}SMA^{-}$, of the venules are $NG2\text{-}\alpha\text{-}SMA^{+}$, and of the arterioles are $NG2^{+}\alpha\text{-}SMA^{+}$. When cultured in vitro, however, pericytes are positive for both of these markers. Other markers that are expressed on both perivascular cell types include calponin and platelet-derived growth factor receptor β (PDGFRβ) (Birukov et al., 1991; Dar et al., 2012).

Examining differences in perivascular cell types is further complicated by added heterogeneities within the subtypes (Hedin and Thyberg, 1987; Kusuma and Gerecht, 2013). Two distinct vSMC phenotypes have been elucidated: synthetic and contractile (Beamish et al., 2010; Hedin and Thyberg, 1987; Wanjare et al., 2013a). Both participate in neovascularization, but synthetic vSMCs predominate in the embryo and in diseased or injured adult vessels while contractile vSMCs predominate in healthy adult vessels.

Human pluripotent stem cells (hPSCs), including human embryonic stem cells (hESCs) and human induced PSCs (hiPSCs), have been widely used to study somatic cell types due to their ability to obtain cell derivatives of identical genetic backgrounds. They are known for their ability to self-renew indefinitely in culture and to differentiate toward every cell type, including perivascular cells (Dar and Itskovitz-Eldor, 2013). hiPSCs are derived from a patient's

own cells and thus can yield derived cell populations that are patient specific, providing a clinically relevant pluripotent cell source for therapeutic use. Indeed, we and others have examined the derivation of both vSMCs (Drukker et al., 2012; Ferreira et al., 2007; Wanjare et al., 2013a) and pericytes (Dar et al., 2012; Kusuma et al., 2013; Orlova et al., 2014).

Using a stepwise differentiation protocol, we have demonstrated the maturation of smooth muscle-like cells (SMLCs) (Vo et al., 2010) to synthetic vSMCs (syn-vSMCs) and contractile vSMCs (con-vSMCs) from both hESCs and hiPSCs (Wanjare et al., 2013a). Using a similar but distinct stepwise differentiation protocol, we have also demonstrated the derivation of pericytes from various hPSC lines (Kusuma et al., 2013).

Building off of our previous studies, we sought to comprehensively define differences among con-vSMCs, syn-vSMCs, and pericytes derived from a common hPSC source in order to uncover cellular and functional differences in vitro, toward the long-term goal of rebuilding vasculature for therapeutic applications. For example, the quality of tissue-engineered blood vessels is dependent on the characteristics of the in vitro perivascular cells used. Current challenges of engineering blood vessels include precise mechanical requirements and tissue-specific cell types (Kumar et al., 2011). The in vitro characterization of our hPSC-derived perivascular cells may mediate the production of tissue-engineered blood vessels that have the patency and mechanical responsiveness equivalent to the native tissue (Chan-Park et al., 2009). Of clinical relevance, the hiPSC-BC1 line is used as the hPSC source for our studies. BC1 is derived without viral integration and has been fully genetically sequenced (Cheng et al., 2012; Chou et al., 2011). Here, we focus on differences in perivascular cells derived from BC1 and hESC H9 cells with respect to cellular characteristics, protein expression, ECM deposition, and remodeling, migration, invasion, and contractility.

RESULTS

Pericytes and vSMCs Differ in Morphological Features and Proliferation Rates

Perivascular cells were derived from hPSCs using differentiation protocols from previous studies (Kusuma et al., 2013; Vo et al., 2010; Wanjare et al., 2013a). Using this protocol, hPSC SMLCs subjected to long-term differentiation and in the presence of high serum and growth factors were guided toward a synthetic fate, whereas deprivation of serum and growth factors yielded a contractile fate (Figure 1A) (Wanjare et al., 2013a). Early pericytes were derived as part of a bicellular population with early ECs named early vascular cells (EVCs) and further differentiated toward mature pericytes by a selective plating strategy (i.e., removal of collagen IV substrate and constrained adhesion time) in the presence of high serum (Figure 1A) (Kusuma et al., 2013). For pericytes, EVCs highly express CD105 and CD146, while pericyte derivatives express NG2, PDGFRβ, CD44, and CD73 (Figure 1A) (Kusuma et al., 2013).

To better understand progression in differentiation, we examined marker expression at different time points along the differentiation of hPSCs. Over the first 6 days of differentiation, the three classes of perivascular cells underwent identical differentiation conditions. During embryonic development, vSMCs may arise from a number of precursors from different germ layers (Cheung et al., 2012; Majesky, 2007). We found that expression of mesodermal genes *KDR*, *APLNR*, and *TCF21* increased over the first 6 days of differentiation in both BC1 and H9 cell lines, whereas expression of neural crest markers *SOX1*, *PAX6*, and *WNT1* remained stagnant (Figure S1A available online). Additionally, *WNT1* was not expressed in BC1 differentiating cells. These data suggest the emergence of a mesodermal population. Furthermore, our day 6 differentiating cells were assessed for the expression of markers indicative of several intermediate lineages: neuroectoderm (nestin), lateral plate mesoderm (KDR), paraxial mesoderm (Pax1) (Cheung et al., 2012), early mesoderm (CD56) (Evseenko et al., 2010), and general mesoderm (CD73) (Boyd et al., 2009; Vodyanik et al., 2010). We found that a small fraction of day 6 differentiating cells was positive for nestin (Figure 1B). KDR was only slightly expressed. Pax1 was not detected via PCR or by immunofluorescence (data not shown). Mesoderm markers CD56 and CD73, however, exhibited more pronounced expression; day 6 differentiating cells were 72% positive for CD56 and >95% positive for CD73. To distinguish the subsequently derived cell populations (i.e., EVCs and SMLCs), we performed flow cytometry analysis for the aforementioned markers. After differentiation toward EVCs, we observed that nestin expression was completely abolished; however, a small fraction of SMLCs remained nestin$^+$ (Figure 1B). Similarly to day 6 differentiating cells, EVCs exhibited >95% positive expression for CD73, whereas CD73 expression decreased to ~70% in SMLCs. An important differentiator between EVCs and SMLCs is the presence of vascular endothelial cadherin (VEcad). Our previous studies demonstrated that BC1-EVCs exhibited approximately 30% VEcad$^+$ cells (Kusuma et al., 2013). Contrastingly, we could not detect VEcad expression on SMLCs (Vo et al., 2010). A similar trend of marker expression was observed at different time points along the differentiation of hESC line H9 (Figure S1B).

We next evaluated the differences in proliferation rates among the hPSC-derived mature perivascular cells. As expected, hiPSC con-vSMCs exhibited low proliferation rates because they are cultured in media containing low serum

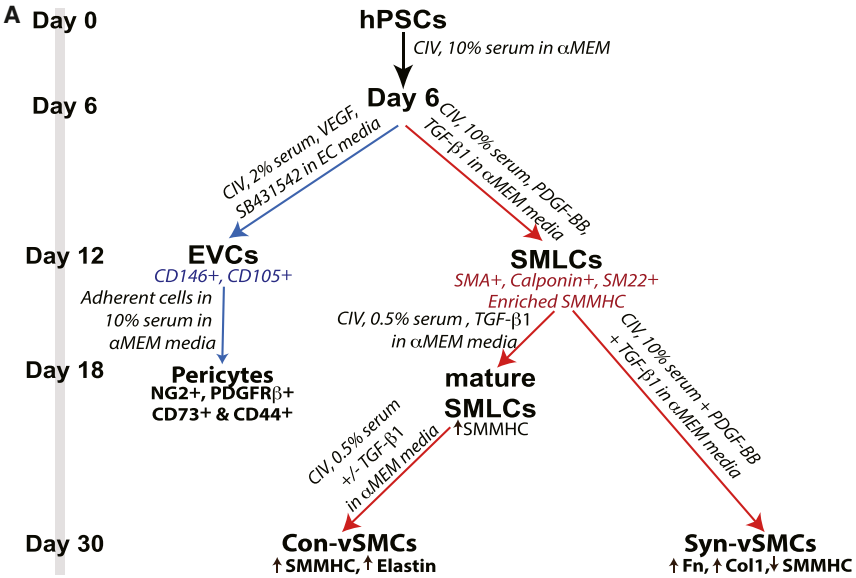

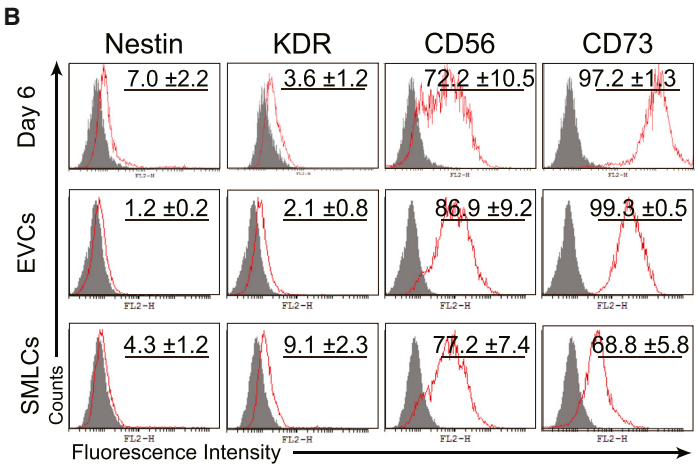

Figure 1. Characterization of Cellular Properties of Perivascular Derivatives

(A) Schema for the differentiation procedure to derive perivascular cells from hPSCs.

(B) Flow cytometry analysis of day 6 differentiating cells, EVCs, and SMLCs. Isotype control in gray. Results shown are representative of three independent experiments. CIV, collagen IV.

See also Figure S1.

(0.5% serum) (Figure 2A) (Wanjare et al., 2013a), while hiPSC syn-vSMCs exhibited high proliferation rates because they are cultured in media containing 10% serum (Figure 2A). Although hiPSC pericytes were cultured using media containing 10% serum, they exhibited contact inhibited proliferation and grew in cell colonies (Figures 2A and 2B). Next, we evaluated the morphological features after culture on 2D surfaces (Figure 2B). While both hiPSC vSMC types spread evenly throughout the Petri dish, hiPSC pericytes arranged themselves into colony-like structures. hiPSC con-vSMCs displayed the largest cell areas and nuclei sizes compared to hiPSC syn-vSMCs and hiPSC pericytes (Figure 2C). hESC derivatives exhibited the same trend (Figure S1C). Indeed, a phenotypic switch from syn-vSMCs to con-vSMCs has been correlated with smaller nuclei and a decrease in proliferation (Chen et al., 1997).

There were stark differences in endoplasmic reticulum (ER), mitochondria location, stress fibers, and the presence of autophagosomes observed between pericytes and vSMCs. As previously described, hiPSC con-vSMCs contain dilated ER, while hiPSC syn-vSMCs contain nondilated ER (Wanjare et al., 2013a) (Figure 2D). On the other hand, hiPSC pericytes (as well as cell-line placental pericytes) contained both dilated and nondilated ER (Figure 2D; Figure S2A). The mitochondria of hiPSC pericytes were in close proximity to the nucleus in contrast to vSMCs, whose mitochondria were located further away from the nucleus. With respect to stress fibers, only con-vSMCs had stress fibers located throughout the entire cell body. Both hiPSC syn-vSMCs and hiPSC pericytes primarily had stress fibers located at the basal lateral surface (Figure 2D). Pericytes also had autophagosomes present, whereas both hiPSC syn-vSMCs and con-vSMCs did not (Figure 2D; Figure S2).

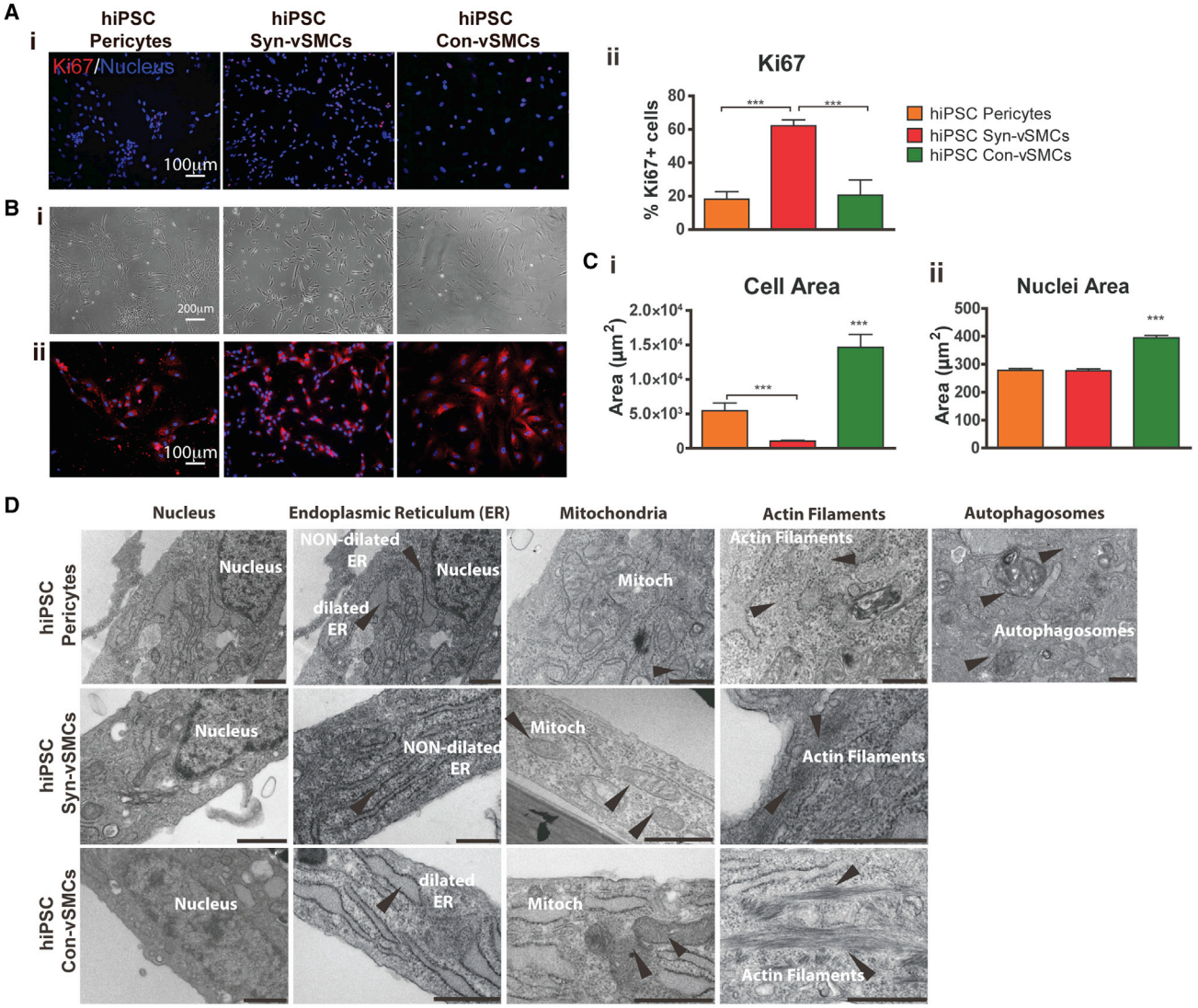

Figure 2. Analysis of hPSC-Derived Perivascular Cells

Derivatives were analyzed for (A) proliferation using (i) stain for Ki67 (red; nuclei in blue) and (ii) corresponding image quantification, (B) morphology using (i) light microscopy and (ii) FM4-64 membrane stain (red) and DAPI (blue), (C) corresponding image quantification of (i) cell and (ii) nuclei area, and (D) subcellular organelle organization using transmission electron microscopy. CIV, collagen type IV; ER, endoplasmic reticulum; mitoch, mitochondria. Scale bars in (D) are 1 μm. Results shown from three independent experiments. All graphical data are reported as mean ± SEM. *p < 0.05, **p < 0.01, and ***p < 0.001. See also Figure S2.

Differential Expression of Perivascular Markers

We next examined the expression and localization of specific cytoskeleton proteins that have been reported to distinguish vSMCs and pericytes. Stress fibers are bundles of actin filaments that are important in mechanotransduction of adherent cells by anchoring to substrates and creating isometric tension (Deguchi et al., 2006). Perivascular cell contraction is associated with a more filamentous cytoskeleton within the cells. Accordingly, the hiPSC con-vSMCs demonstrated elevated stress fibers per cell compared to both hiPSC syn-vSMCs and hiPSC pericytes, which had significantly fewer stress fibers per cell (Figure 3A, i and ii; additional fields of view in Figure S3). While differences in α-SMA expression and organization could not be observed, calponin expression was upregulated in hiPSC pericytes (Figure 3A, i and iii; Figure S3).

The cell-surface proteins NG2 and PDGFRβ are also commonly associated with perivascular cells. The proteoglycan NG2 has been shown to be widely expressed by perivascular cells in both vasculogenic and angiogenic vasculature (Ozerdem et al., 2001). While NG2 is an appropriate marker for identifying pericytes in microvessels, it is

merely a supplemental vSMC identifier considering the variety of vSMC markers (Ozerdem et al., 2001). Interestingly, profuse stress fibers were observed with the expression of NG2 protein only in hiPSC con-vSMC cultures (Figure 3B, i). Indeed, NG2 mRNA expression in hiPSC con-vSMCs was significantly elevated compared to hiPSC syn-vSMCs and hiPSC pericytes (Figure 3B, ii). Similarly, aortic vSMCs exhibited NG2 expression with profuse stress fibers compared to placental pericytes (Figure 3B, ii; Figure S4A). We observed differences in the expression of PDGFRβ in our hiPSC derivatives. hiPSC con-vSMCs exhibited elevated PDGFRβ mRNA expression that had a punctuate membrane expression as well as nuclear expression (Figure 3C, i and ii) comparable to aortic vSMCs (Figure S4B).

The mature vSMC marker SMMHC is associated with the contractile vSMC phenotype (Babu et al., 2000; Patel et al., 2006). hiPSC con-vSMCs exhibited elevated SMMHC expression compared to hiPSC syn-vSMCs and pericytes (Figure 3C). Correspondingly, aortic vSMCs exhibited elevated SMMHC expression and SMMHC stress fibers, while placental pericytes did not (Figure 3C; Figure S4B). We further evaluated mRNA and protein expression of SMMHC on our perivascular cell derivatives. hiPSC con-vSMCs exhibited the greatest expression of SMMHC mRNA compared to all other cell types tested (Figure 3C, ii). At the protein level, SMMHC was only detected on control aortic vSMCs and hiPSC con-vSMCs (Figure 3C, iii); hiPSC syn-vSMCs were negative for SMMHC. Interestingly, SMMHC was not detected in either hiPSC pericytes or control placental pericytes (Figure 3C, ii and iii). Finally, the expression of caldesmon, which plays an important role in the perivascular contraction function, was assessed in the different types of perivascular cells. We found that caldesmon was elevated in con-vSMCs compared to syn-vSMCs and pericyte derivatives (Figure 3D). We note that the expression of perivascular markers in aortic vSMCs cultured in low serum (0.5%) conditions was slightly altered yet exhibited a similar trend of aortic vSMCs cultured in 10% serum and hiPSC con-vSMCs (Figure S4C).

ECM Protein Production

A primary function of perivascular cells is the deposition of ECM proteins to help stabilize vasculature. Because the ECM composition of various vessel types differs, we next assessed the different perivascular cell types for expression and production of ECM proteins collagen I, collagen IV, fibronectin, laminin, and elastin in vitro (Figure 4). We found that both phenotypes of vSMCs exhibited concentrated perinuclear collagen I expression, while hiPSC pericytes demonstrated diffuse expression of collagen I around the cytoplasm (Figure 4A, i). hiPSC syn-vSMCs and hiPSC pericytes exhibited similar extracellular and globular expression of collagen IV, while hiPSC con-vSMCs had abundant fibrous intracellular and extracellular collagen IV (Figure 4A, ii). hiPSC con-vSMCs deposited abundant fibronectin extracellularly (Figure 4A, iii); though abundant fibronectin production was detected by hiPSC syn-vSMCs and pericytes, we observed fibronectin production was primarily intracellular (Figure 4A, iii). Laminin appeared perinuclearly around the three perivascular derivatives (Figure 4A, iv). However, hiPSC pericytes exhibited a punctate expression compared to the diffuse laminin protein expression in vSMC derivatives (Figure 4A, iv). Comparable deposition of ECM proteins was observed in aortic vSMCs and placental pericytes (Figure S5A).

A mature vSMC marker implicated in the mechanical responsiveness of vSMCs (Babu et al., 2000; Patel et al., 2006), elastin was expressed primarily intracellularly and diffusely within con-vSMCs, with some cells exhibiting perinuclear characteristic disordered elastin expression (Figure 4A, v). Correspondingly, aortic vSMCs exhibited elastin expression with both intracellular and extracellular deposition (Figure S5B). We could not detect elastin in either hiPSC syn-vSMCs, or hiPSC pericytes (Figure 4A, v).

Corroborating our immunofluorescence data, we performed RT-PCR analysis on the tested perivascular cells (Figure 4B). We found an increased expression of collagens I and IV and elastin by hiPSC con-vSMCs. Surprisingly, hiPSC pericytes demonstrated the highest expression of fibronectin and its extra domain A (ED-A fibronectin; Figure S5C), suggesting the propensity of the derived pericytes to produce fibronectin under amenable in vitro culture conditions. hiPSC con-vSMCs had higher levels of both fibronectin and ED-A fibronectin than syn-vSMCs. Con-vSMCs and aortic vSMCs exhibited the greatest expression of both laminin and elastin compared to the other tested perivascular cell types. Interestingly, aortic vSMCs had lower expression of collagen I compared to hiPSC con-vSMCs; placental pericytes exhibited lower expression of collagen IV and fibronectin compared to hiPSC pericytes (Figure 4B; Figure S5C). Finally, the hiPSC con-vSMCs expressed elastin mRNA 100-fold more than the hiPSC syn-vSMCs and hiPSC pericytes (Figure 4B). We note that elastin expression in aortic vSMCs was higher compared to hiPSC con-vSMCs and increased when aortic vSMCs were cultured in low serum, demonstrating the importance of culture conditions for the derivation of perivascular cell types from hiPSCs (Figure 4B; Figure S5D).

In the vasculature, there exists a wide range of matrix metalloproteinases (MMPs), which are proteolytic enzymes that degrade the ECM and remodel the architecture of associated vessels. The degradation of ECM allows perivascular cells to migrate and proliferate (Raffetto and Khalil, 2008). Via zymography analysis, we found that only hiPSC syn-vSMCs produce pro-MMP9. Both hiPSC syn-vSMCs and

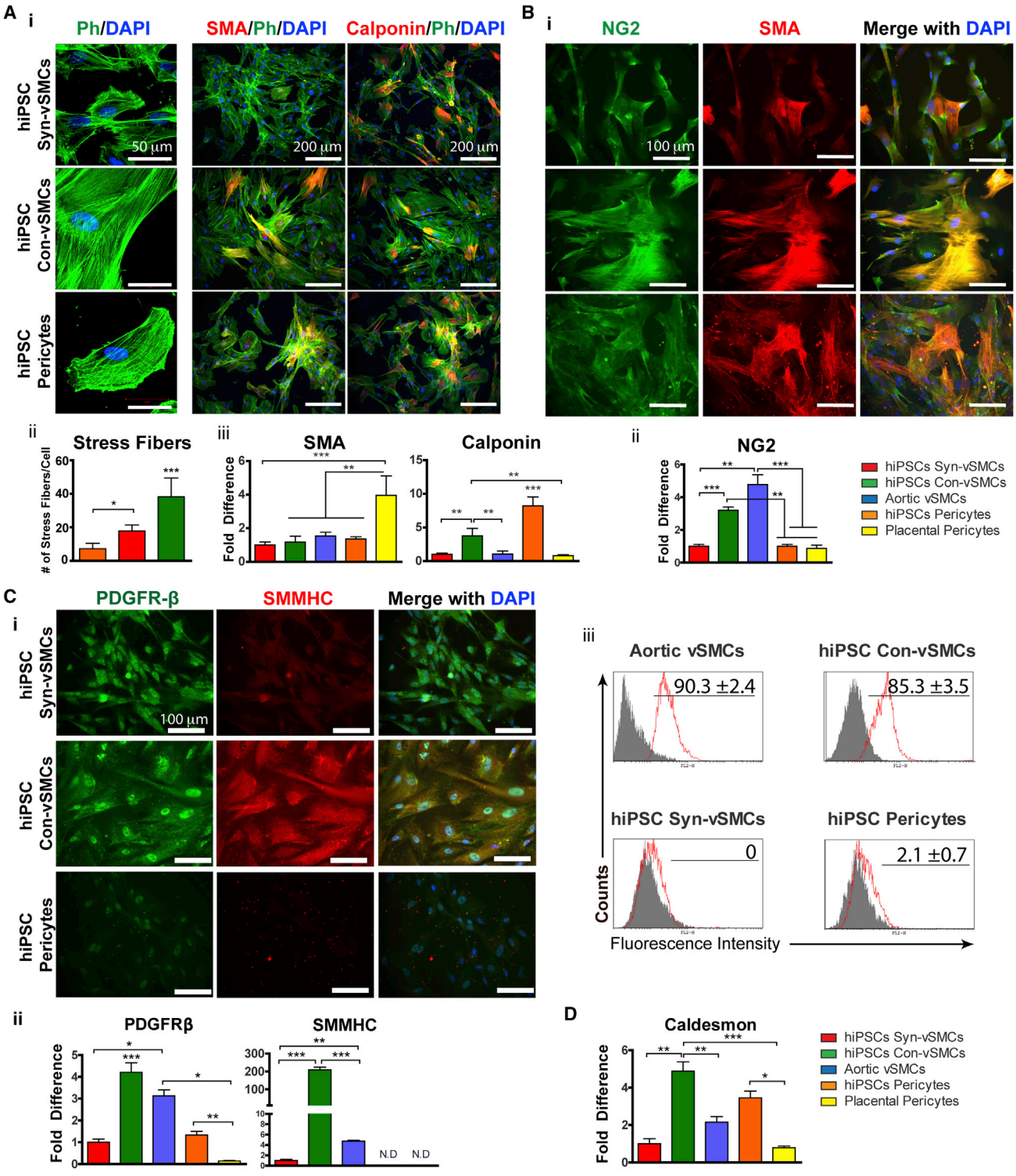

Figure 3. Differences in Stress Fiber and Contractile Marker Expression

Perivascular derivatives were assessed for (A) (i) organization of stress fibers (confocal z-stacks), α-SMA, and calponin (in red; phalloidin in green; nuclei in blue); (ii) stress fiber number and (iii) α-SMA and calponin expression via quantitative real time RT-PCR; (B) (i) organization of NG2 (green) and α-SMA (red; nuclei in blue) and (ii) NG2 expression using quantitative real-time RT-PCR; (iii) (C) (i)

(legend continued on next page)

hiPSC pericytes produce pro-MMP2 and its active form, while hiPSC con-vSMCs produce only the pro-MMP2 (Figure 4C, i). We could not detect MMP1 expression using zymography (data not shown). Molecular analysis revealed that hiPSC pericytes have greater *MMP14* mRNA expression, while syn-vSMCs have the lowest expression (Figure 4C, ii).

Functionality

In the body, the cellular dynamics of perivascular cells can provide information regarding whether a vessel is emergent, pathogenic, remodeling, or at a stable steady state. Of particular functional importance are multipotency, in vivo behavior, migration, invasion, and contractility of perivascular cells.

Multipotency

A major feature of pericytes is their ability to behave as mesenchymal precursors (Crisan et al., 2008). Indeed, our previous studies have demonstrated that pericyte derivatives could be differentiated to adipocytes and osteoblasts (Kusuma et al., 2013). Contrastingly, neither hiPSC con-vSMCs nor syn-vSMCs demonstrated the potential to differentiate toward adipogenic or osteogenic lineages (Figure 5A).

In Vivo Integration

To compare in vivo functionality, we employed a Matrigel plug assay using our hiPSC perivascular cells. After 1 week of subcutaneous transplantation, all three types of perivascular cells aligned next to the host's growing functional vasculature, with occasional circumferential wrapping observed by con-vSMCs and pericytes (Figure 5B) and vascular tube narrowing observed only by con-vSMCs (Kusuma et al., 2013; Wanjare et al., 2013a).

Migration

Mechanisms that induce cell motility include chemokinesis, chemotaxis, responses to interactions with ECM, and random increases such as in wound healing (Louis and Zahradka, 2010). In a wound-healing assay, hiPSC pericytes and hiPSC syn-vSMCs migrated inward from the wound margin (Figure 5C, i). hiPSC pericytes exhibited a significant number of trajectories that were not perpendicular to the wound margin, whereas hiPSC con-vSMCs followed oriented trajectories predominantly toward the right. Indeed, after 24 hr, wound closure was observed only with the hiPSC syn-vSMCs (Figure 5C, i and ii). Overall, the hiPSC con-vSMCs exhibited the slowest migration speed (Figure 5C, iii).

Invasion

Invasion is the cell motility associated with ECM degradation. To assess the ability of perivascular cells to invade toward ECs, we cultured a monolayer of ECs beneath a 3D collagen gel. Each perivascular cell type was cultured atop the collagen gel, and migration was measured after 48 hr. Human iPSC syn-vSMCs exhibited increased invasion toward ECs after 48 hr compared to hiPSC con-vSMCs and hiPSC pericytes (Figure 5D, i). Quantification of this dynamic behavior further revealed not only that more hiPSC syn-vSMCs invaded the collagen gels compared to the other perivascular cells but also that they invaded to a deeper distance (Figure 5D, ii and iii).

Contractility

In healthy blood vessels, perivascular cells provide stability to vessels by contracting to counteract the pulsatile force generated by heartbeats. Examining the contractility of the three perivascular derivatives in response to the cholinergic agonist drug carbachol, we found that hiPSC con-vSMCs contracted significantly more than both hiPSC pericytes and hiPSC syn-vSMCs (Figure 5E).

DISCUSSION

The major function of both pericytes and vSMCs is to stabilize blood vessels, and thus both exhibit a great deal of similarities. Distinguishing among the three perivascular cells will facilitate their use in tissue engineering applications. Because pericytes are found in capillaries (<10 μm diameter) and microvessels (10–100 μm diameter), while vSMCs are found in larger vessels (>100 μm diameter), we sought to investigate methods that could elucidate similarities and differences between pericytes and vSMCs in vitro.

In previous studies, we derived pericytes (Kusuma et al., 2013) and both hiPSC syn-vSMCs and hiPSC con-vSMCs (Wanjare et al., 2013a). In performing direct comparisons between these perivascular cell derivatives, we observed numerous differences that enable the study of human perivascular development and functionality and may shed light on means to not only distinguish between them but also clearly define their functionality for future use in tissue-regenerative strategies. A summary of the key features compared among the perivascular derivatives from hiPSC-BC1 is shown in Table 1.

By assessing marker expression from day 6 differentiating cells compared to derived EVCs and SMLCs, we were able to label our day 6 cells as early mesoderm, characterized by

PDGFRβ (green) and SMMHC (red; nuclei in blue) and (ii) PDGFRβ and SMMHC expression using quantitative real-time RT-PCR; (iii) flow cytometry analysis of SMMHC (isotype control in gray); and (D) caldesmon expression via quantitative real-time RT-PCR. Results shown from three independent experiments; each RT-PCR sample was run with three technical replicates. All graphical data are reported as mean ± SEM. *$p < 0.05$, **$p < 0.01$, and ***$p < 0.001$. See also Figures S3 and S4.

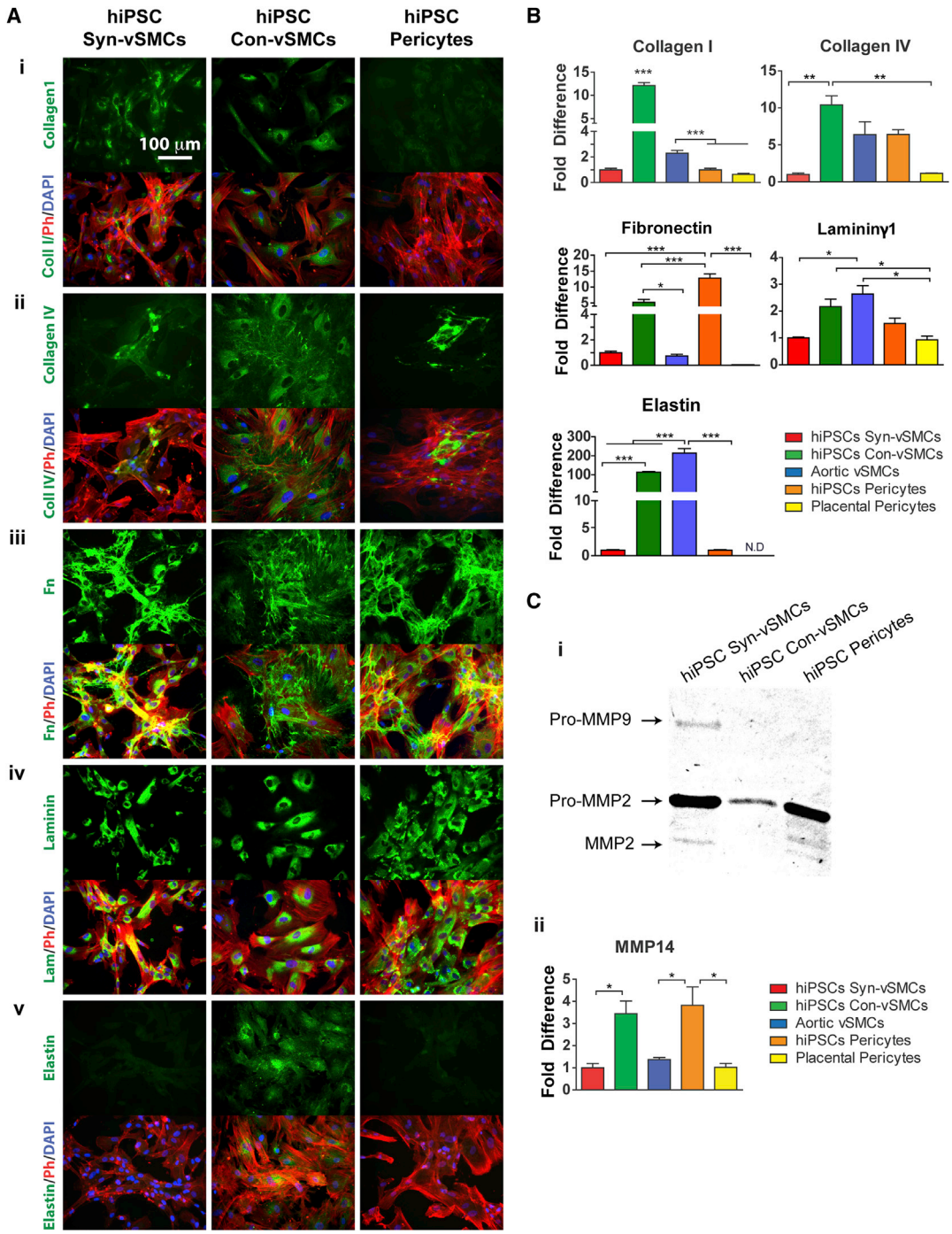

Figure 4. Differential ECM and MMP Expression by Perivascular Derivatives

(A and B) Perivascular derivatives were examined for the production of ECM proteins (i) collagen I, (ii) collagen IV, (iii) fibronectin, (iv) laminin, and (v) elastin (all in green; phalloidin in red; nuclei in blue) after 6 days in culture (A), and their relative expression via quantitative real-time RT-PCR is shown (B).

(C) Perivascular derivatives were compared for (i) the production of MMP2 and MMP9 using zymography, and (ii) the relative expression of *MMP14* using quantitative real-time RT-PCR is shown.

Results from three independent experiments are shown; each RT-PCR sample was run with three technical replicates. All graphical data are reported as mean ± SEM. *$p < 0.05$, **$p < 0.01$, and ***$p < 0.001$.

See also Figure S5.

expression of CD56 and CD73. Via EVC differentiation, day 6 cells differentiate into VEcad$^+$ and PDGFRβ$^+$ cells (Kusuma et al., 2013); in SMLC differentiation, day 6 cells were induced to differentiate into cells positive for SMMHC, SM22, and calponin (Vo et al., 2010).

In vivo perivascular cell characteristics are dependent on the local 3D cellular environment, which is composed of cell-cell interactions, surrounding ECM, local mechanical conditions, and chemical cues. While contractile vSMCs are quiescent in the body, synthetic vSMCs display increased proliferation in order to remodel vessels in response to growth factors and cytokines released during vessel injury or disease (Sprague and Khalil, 2009). The in vitro cell culture supplement, serum, contains numerous cytokines and growth factors among other chemokines such as hormones, lipids, attachment factors, etc. (Brunner et al., 2010). Therefore, hiPSC syn-vSMCs responded in vitro just as the synthetic phenotype in the body with high proliferation rates as they were exposed to these different chemokines in serum. Although endothelial-pericyte interactions have been studied extensively, pericyte-pericyte interactions are not well understood. Here, we show the colony-like growth of hiPSC pericytes, suggesting that profound gap junction interactions are needed to activate contact inhibited proliferation of our hiPSC pericytes (Li et al., 2003).

The ER is a major organelle involved in cell protein synthesis. Although in vivo synthetic rat vSMCs have been shown to increase their secretory apparatus that included extensive active ER and Golgi complexes compared to contractile vSMCs, in vitro we observe significant differences in ER size (Thyberg et al., 1997). An in vivo study using mice with knockout miR-143 and miR-145, microRNAs that promote the contractile vSMC phenotype, reported that mice aortas exhibited synthetic vSMC phenotypes and dilated ER containing flocculent material (Elia et al., 2009). In contrast, we show in vitro that hiPSC con-vSMCs have dilated ER, hiPSC syn-vSMCs have nondilated ER, and hiPSC pericytes have both types of ER. Expansion of the ER in mammalian cells has been reported to be necessary in order to accommodate increasing luminal content (mostly unfolded proteins) as a result of ER stress or improper ER function (Görlach et al., 2006; Schönthal 2012). Consequently, the observed ER expansion may indicate that serum deprivation activates vSMC contraction signaling while halting ER-dependent protein synthesis, folding, and transport signaling, thus creating a bottleneck in the ER machinery and giving rise to the dilated appearance. Because their ER machinery is a low priority, hiPSC con-vSMCs therefore have accumulated unfolded proteins in their dilated ER and are functionally dedicated to cell contractility. Likewise, ER stress in the endothelium has also been linked to the increased contraction of isolated mouse aortas (Liang et al., 2013). Liang et al. demonstrated that there was greater phenylephrine-induced vasoconstriction in the aortas of AMP-activated protein kinase knockout mice (AMPKα2$^{-/-}$), which exhibit aberrant ER stress in ECs compared to WT mice (Liang et al., 2013). The study may suggest that vSMCs not only functionally contract more as a result of their own ER stress, but may also respond in a similar manner in response to EC ER stress. This correlation between ER stress and vSMC contractility may additionally have a role in vessel diseases such as atherosclerosis in which vSMCs take on a synthetic phenotype and contraction is greatly reduced (Rzucidlo et al., 2007). For instance, apoptosis of vSMCs as a result of vSMC ER stress has been implicated in collagen production in atherosclerotic lesions (Tabas, 2010). Therefore, differences in ER signaling cues as well ER structure in our hiPSC con-vSMCs and hiPSC syn-vSMCs may be helpful in studying the diseased syn-vSMCs in vitro. Finally, the proximity of mitochondria to the nucleus as well as the presence of autophagosomes in both placental and hiPSC pericytes, but not in hiPSC vSMCs, may also indicate differences in the cellular machinery of pericytes.

We also found clear differences in the amount of stress fibers between the perivascular derivatives. Abundant stress fibers were found in con-vSMCs located throughout the entire cell body. While hiPSC syn-vSMCs had fewer stress fibers, pericyte derivatives demonstrated the lowest levels of stress fibers per cell and had stress fibers located at the basal lateral surface. All perivascular cells expressed α-SMA in similar levels while calponin was found to be highly expressed in hiPSC pericytes, suggesting that this typical early vSMC marker may also be helpful to identify pericytes. Our findings also indicate that SMMHC is a distinctive marker for con-vSMCs. Upregulated expression and stress fiber organization of SMMHC were observed in hiPSC con-vSMCs. The markers NG2 (or CSPG4) and PDGFRβ are widely utilized to identify pericytes; however, vSMCs also express these markers, making it difficult to distinguish which cell type is actually represented (Murfee et al., 2005). NG2 has been observed to be expressed by both pericytes and vSMCs in arterioles and capillaries, but not beyond postcapillaries (along venules), in rats (Murfee et al., 2005). Here, we showed that con-vSMCs can be distinguished from pericytes and syn-vSMCs by colocalization of NG2 with stress fibers.

The in vitro production and expression of ECM proteins collagens I and IV and laminin differed between the perivascular derivatives. In the body, pericytes produce ECM in the subendothelial basement membrane of capillaries, while both vSMCs and pericytes produce ECM in the tunica media layer of larger blood vessels (Niland, 2009). Collagen I, a fibrillar collagen, is a substantial component of the interstitial connective tissue in contrast to collagen

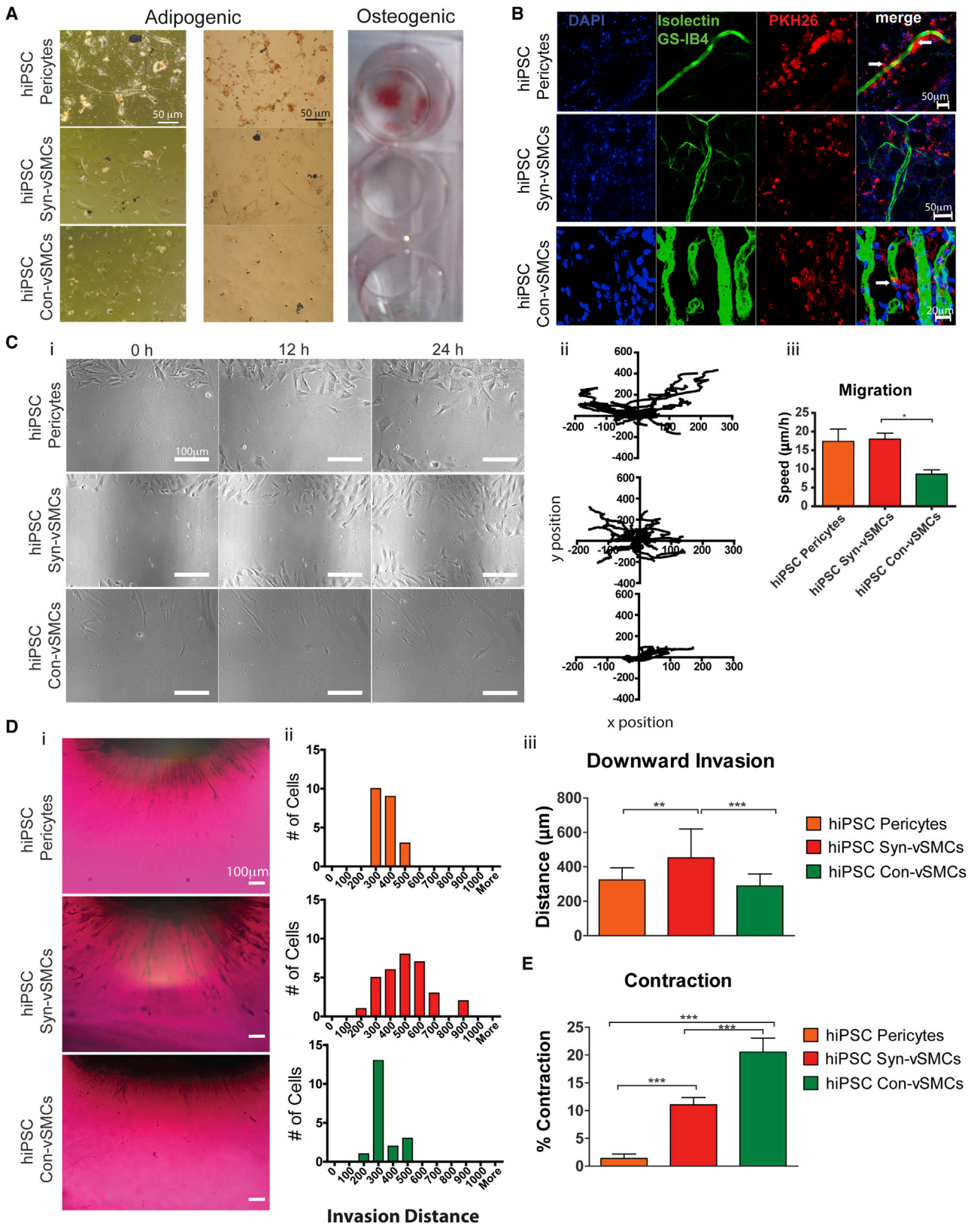

(legend on next page)

Table 1. Summary of Features Compared among hPSC-Derived Perivascular Cells

Cell Type/Features	Con-vSMCs	Syn-vSMCs	Pericytes
Morphology	large, spindle-like	small, spindle-like	colony-like, flat, polygonal
Proliferation rate	+	+++	+
Cell size	+++	++	+
Endoplasmic reticulum	dilated	nondilated	dilated+ nondilated
Markers	SMA, calponin, NG2, PDGFRβ, SMMHC	SMA, calponin, NG2, PDGFRβ, $SMMHC^{low}$	SMA, calponin NG2, PDGFRβ
ECM mRNA expression	collagen I^{high}, collagen IV^{high}, fibronectin, laminin	collagen I, collagen IV, fibronectin, laminin	collagen I, collagen IV, $fibronectin^{high}$, laminin
ECM deposition	collagen I, collagen $IV^{fibrous}$, fibronectin, $laminin^{diffuse}$, elastin	collagen I^{low}, collagen $IV^{globular}$, fibronectin, $laminin^{diffuse}$	collagen $IV^{globular}$, fibronectin, $laminin^{punctuate}$
MMPs	14 (MT-1)	2, 9	2, 14
Mesenchymal differentiation	—	—	adipogenic, osteogenic
In vivo integration	alignment, circumferential wrapping, tube narrowing	alignment	alignment, circumferential wrapping
Migration	−/+	+++	++
Invasion	−/+	+++	+
Contractility	+++	+	−/+

Note that values are relative to the three cell types examined.

IV, which is present in all basal lamina, forming the basic irregular fibrous 2D network of vasculature (Eble and Niland, 2009). Similarly, laminin is an indispensible component of the vascular basement membrane, the primary site where collagen IV and laminin form an interdependent network (Eble and Niland, 2009). In human arteries, collagen I, deposited between vSMCs, was reported to exhibit sparse thin fiber morphology in the media of small arteries while being organized in fibrillar structures in larger arteries. We report that in vitro, hiPSC pericytes, associated with small vasculature, have a greatly diminished collagen I expression compared to both hiPSC syn-vSMCs and hiPSC con-vSMCs, found in larger vessels (Shekhonin et al., 1987). Both our in vitro findings and in vivo studies illustrate that perivascular cells associated with larger vessels express more collagen I. From our in vitro study, we also observed that a morphologically distinct high density globular collagen IV expression is deposited by both hiPSC syn-vSMCs and pericytes, while a more fibrous collagen IV deposition as well as increased collagen IV expression is exhibited by hiPSC con-vSMCs. Similarly, in vivo, collagen IV deposition varies between the two phenotypes of vSMCs. For instance, fibrous plaques of atherosclerotic human arteries, known to mainly contain syn-vSMCs, have been reported to have greatly decreased collagen IV deposition and increased collagen I

Figure 5. Comparison of Functionalities Demonstrated by Perivascular Derivatives

(A) Differentiation potential of perivascular derivatives into mesenchymal lineages including adipocytes (oil red O stain) and osteoblasts (alizarin red S stain).

(B) One-week subcutaneously transplanted perivascular derivatives (in red; PKH26) migrated to newly formed host blood vessels (mouse ECs in green [Alexa 488-conjugated isolectin IB4]) within Matrigel, as indicated by representative confocal images. White arrows indicate occasions of circumferential wrapping of vasculature by the transplanted hiPSC derivatives; nuclei are indicated in blue (DAPI).

(C) Migration potential via a wound-healing assay. Shown are (i) phase-contrast images quantified for (ii) cell trajectories and (iii) speed.

(D) Downward invasion of hiPSC perivascular cells through collagen gels toward ECs was examined after 48 hr via (i) cross section of toluidine blue-dyed cells and (ii) quantification of the cell number, distance of invasion, and (iii) the average distance traveled.

(E) Contraction was induced by 10^{-5} M carbachol, and percent contraction was quantified.

Results shown from at least three biological replicates using three independent fields of view in each. All graphical data are reported as mean ± SEM. *$p < 0.05$, **$p < 0.01$, and ***$p < 0.001$.

deposition around vSMCs compared to healthy arteries containing contractile vSMCs (Rekhter, 1999; Shekhonin et al., 1985, 1987). However, the loci of the plaques have been shown to have large quantities of collagen IV, correlating with the vSMCs being surrounded by layers of basement membrane material in this region (Rekhter, 1999; Shekhonin et al., 1987). Additionally, the in vitro laminin expression was different in hiPSC pericytes compared to both phenotypes of hiPSC vSMCs. hiPSC con-vSMCs had diffuse cytoplasmic expression of laminin, while hiPSC pericytes had punctate expression around the cell membrane. hiPSC syn-vSMCs had mostly diffuse cytoplasmic expression of laminin with few instances of punctate expression. In vivo, rat synthetic vSMCs lost the ability to produce laminin unlike contractile vSMCs (Thyberg et al., 1997). Fibronectin was expressed and deposited by all tested perivascular cell types, with hiPSC pericytes expressing the highest fibronectin mRNA levels. Human iPSC con-vSMCs expressed higher levels of fibronectin mRNA compared to hiPSC syn-vSMCs. Similarly, the hiPSC con-vSMCs also expressed higher levels of ED-A fibronectin compared to the hiPSC syn-vSMCs, while in vivo, ED-A fibronectin was suggested to be associated with the synthetic phenotype (Glukhova et al., 1989). Examination of the expression pattern of ED-A fibronectin in differentiating stem cells highlights the need for further investigation of stem cell derivatives and the conceivable differences between in vitro and reported in vivo phenotypes, thus warranting additional studies correlating fibronectin slice variants to perivascular phenotypes both in vitro and in vivo. Elastin was also highly expressed by con-vSMCs compared to all other perivascular cell types. Not only is elastin production characteristic of the contractile phenotype, but also, interestingly, in vivo studies demonstrated that increasing elastin production itself promoted a contractile vSMC phenotype by inhibiting vSMC proliferation (Karnik et al., 2003; Urbán et al., 2002).

Pericytes and vSMCs have been known to express the gelatinases MMP2 and MMP9 needed to degrade basement membranes during vessel remodeling (Candelario-Jalil et al., 2009; Newby, 2006; Virgintino et al., 2007). Accordingly, in vitro, hiPSC syn-vSMCs expressed MMP2 and MMP9, corresponding to previous observations that this phenotype is associated with vessel remodeling, which includes ECM degradation. The expression of MMP2 and MMP9 in hiPSC pericytes coincided with pericytes' close contact with basement membranes of vessels. A membrane-associated MMP, *MMP14*, was more greatly expressed by derived pericytes compared to control placental pericytes. MMP14 is known for its ability to degrade various ECM proteins; thus, we had expected that control pericytes would express this MMP type more greatly given the abundance of these ECM proteins in microvessels and capillaries. We suspect the discrepancy may be due to a loss of this site-specific feature due to in vitro culture of harvested pericytes, emphasizing the advantages of derived perivascular cell types over primary cells.

Not surprisingly, only hiPSC-derived pericytes had the potential to differentiate to mesenchymal lineages, including adipogenic and osteogenic, while neither hiPSC nor vSMC types could differentiate. In vivo, all transplanted perivascular cells aligned next to the host vasculature, with both pericytes and con-vSMCs occasionally wrapping the microvasculature. These differences correlated with in vivo phenotypes of these various perivascular cell types; both pericytes and con-vSMCs support vasculature in vivo and are thus closely associated with the endothelial lining, providing support. Syn-vSMCs, alternatively, are known for their role in remodeling vasculature. Differences in cellular mechanics may also be used to distinguish among the three different perivascular cell types. hiPSC syn-vSMCs were able migrate in response to wounding and invade through ECM toward ECs, whereas hiPSC con-vSMCs were not. Interestingly, while the hiPSC pericytes migrated in response to wounding, they failed to invade through ECM toward ECs, indicative of their short-distance migratory nature. This result coincides with the fact that pericytes have a close spatial relation to ECs in vessels (Díaz-Flores et al., 2009).

Finally, hiPSC con-vSMCs can be characterized by their elevated cellular contractility (as demonstrated by both carbachol treatment and increased expression of contractile protein [caldesmon]), while hiPSC syn-vSMCs are characterized by increased speed, migration, and invasion. These results are in agreement with previous observations that vSMCs switch to a synthetic phenotype in the body in response to injury to aid in tissue repair (Louis and Zahradka, 2010).

In summary, these perivascular derivatives demonstrate an important building block toward not only reconstructing physiologically relevant vasculature but also the study of developmental processes and diseases implicating these cell types. Important elements of our system are the several noted discrepancies between our in vitro results and in vivo phenotypes, alluding to the complexity of the field. A major challenge of correlating in vitro results to phenotypes observed in vivo is the presence of heterogeneous vSMC subpopulations of unknown origin that lie between the contractile and synthetic phenotypic spectrum in vivo. Unanswered questions, particularly those regarding the in vivo synthetic phenotype, still remain. For instance, ECM deposition of syn-vSMCs located in vastly different environments such as normal developing or remodeling vessels compared to diseased or injured vessels remains

unknown. To further add to the complication, by utilizing SMMHC lineage tracing, Tang et al. reported that synthetic vSMCs actually arise from multipotent stem cells lying within vessels and not phenotypic switching by vSMCs in vivo (Drukker et al., 2012; Tang et al., 2012). The advantage of our study is the derivation and comparison of synthetic and contractile vSMCs from a known common early smooth muscle precursor. In fact, some of our study's in vitro results actually yield a more useful phenotype for engineering blood vessels, such as increased ECM production from the hiPSC derivatives compared to control cell lines; however, other discrepancies, such as lower expression of fibronectin splice variant ED-A in derived syn-vSMCs compared to con-vSMCs, drive the need for continued study on the derivation of specialized cell types to rebuild tissue. Additionally, studies in a 3D environment would allow further investigation of morphological features such as nucleic size that may better match in vivo properties.

Overall, the ability to generate human perivascular cells including contractile vSMCs, synthetic vSMCs, and pericytes with identical genetic backgrounds offers unprecedented opportunities to study the development and functionality of well-defined human perivascular derivatives from healthy and disease hiPSCs. Furthermore, by employing a viral integration-free and fully genetically sequenced hiPSC line, BC1, we anticipate that these findings hold translational importance.

EXPERIMENTAL PROCEDURES

Complete experimental procedures are available online (see the Supplemental Experimental Procedures).

Cell Culture

hiPSC Line and Differentiation

The hiPSC line BC1 (Cheng et al., 2012; Chou et al., 2011; kindly provided by Dr. Cheng, SOM JHU) and the hESC line H9 were expanded and differentiated to perivascular cells as described previously (Kusuma et al., 2013; Wanjare et al., 2013a).

Stress Fiber Quantification

The number of stress fibers per cell was quantified using line intensity profiles of cells in ImageJ (Wei et al., 2011). Stress fibers were labeled with fluorescent Alexa 488 phalloidin and imaged at 20× and 40×. A line-intensity profile across a single cell was generated, with each peak representing a single stress fiber.

Invasion toward ECs

A downward invasion assay was used to assess invasion of perivascular cells. Human umbilical vein ECs were seeded on 16-well detachable wells (Fisher). After 24 hr, 150 μl of collagen gel (150 μl) was added on top of the ECs. After 1 hr, hiPSCs perivascular cells were seeded on top of the gels. After 48 hr, the gels were fixed and stained with toluidine blue dye and cross sections of the gels were imaged and quantified.

SUPPLEMENTAL INFORMATION

Supplemental Information includes five figures and Supplemental Experimental Procedures and can be found with this article online at http://dx.doi.org/10.1016/j.stemcr.2014.03.004.

ACKNOWLEDGMENTS

We gratefully acknowledge support for this work by a NIH predoctoral award from NIH grant F31HL112644 (to S.K.) and NIH grant R01HL107938 (to S.G).

Received: October 11, 2013
Revised: March 12, 2014
Accepted: March 13, 2014
Published: April 17, 2014

REFERENCES

Alberts, B., Johnson, A., Lewis, J., Raff, M., Roberts, K., and Walter, P. (2002). Molecular Biology of the Cell, Fourth Edition (New York: Garland Science).

Babu, G.J., Warshaw, D.M., and Periasamy, M. (2000). Smooth muscle myosin heavy chain isoforms and their role in muscle physiology. Microsc. Res. Tech. *50*, 532–540.

Beamish, J.A., He, P., Kottke-Marchant, K., and Marchant, R.E. (2010). Molecular regulation of contractile smooth muscle cell phenotype: implications for vascular tissue engineering. Tissue Eng. Part B Rev. *16*, 467–491.

Birukov, K.G., Stepanova, O.V., Nanaev, A.K., and Shirinsky, V.P. (1991). Expression of calponin in rabbit and human aortic smooth muscle cells. Cell Tissue Res. *266*, 579–584.

Boyd, N.L., Robbins, K.R., Dhara, S.K., West, F.D., and Stice, S.L. (2009). Human embryonic stem cell-derived mesoderm-like epithelium transitions to mesenchymal progenitor cells. Tissue Eng. Part A *15*, 1897–1907.

Brunner, D., Frank, J., Appl, H., Schöffl, H., Pfaller, W., and Gstraunthaler, G. (2010). Serum-free cell culture: the serum-free media interactive online database. ALTEX *27*, 53–62.

Candelario-Jalil, E., Yang, Y., and Rosenberg, G.A. (2009). Diverse roles of matrix metalloproteinases and tissue inhibitors of metalloproteinases in neuroinflammation and cerebral ischemia. Neuroscience *158*, 983–994.

Chan-Park, M.B., Shen, J.Y., Cao, Y., Xiong, Y., Liu, Y., Rayatpisheh, S., Kang, G.C.-W., and Greisler, H.P. (2009). Biomimetic control of vascular smooth muscle cell morphology and phenotype for functional tissue-engineered small-diameter blood vessels. J. Biomed. Mater. Res. A *88*, 1104–1121.

Chen, Y.-H., Chen, Y.-L., Lin, S.-J., Chou, C.-Y., Mar, G.-Y., Chang, M.-S., and Wang, S.-P. (1997). Electron microscopic studies of phenotypic modulation of smooth muscle cells in coronary arteries of patients with unstable angina pectoris and postangioplasty restenosis. Circulation *95*, 1169–1175.

Cheng, L., Hansen, N.F., Zhao, L., Du, Y., Zou, C., Donovan, F.X., Chou, B.K., Zhou, G., Li, S., Dowey, S.N., et al.; NISC Comparative Sequencing Program (2012). Low incidence of DNA sequence variation in human induced pluripotent stem cells

generated by nonintegrating plasmid expression. Cell Stem Cell *10*, 337–344.

Cheung, C., Bernardo, A.S., Trotter, M.W.B., Pedersen, R.A., and Sinha, S. (2012). Generation of human vascular smooth muscle subtypes provides insight into embryological origin-dependent disease susceptibility. Nat. Biotechnol. *30*, 165–173.

Chou, B.K., Mali, P., Huang, X., Ye, Z., Dowey, S.N., Resar, L.M.S., Zou, C., Zhang, Y.A., Tong, J., and Cheng, L. (2011). Efficient human iPS cell derivation by a non-integrating plasmid from blood cells with unique epigenetic and gene expression signatures. Cell Res. *21*, 518–529.

Crisan, M., Yap, S., Casteilla, L., Chen, C.W., Corselli, M., Park, T.S., Andriolo, G., Sun, B., Zheng, B., Zhang, L., et al. (2008). A perivascular origin for mesenchymal stem cells in multiple human organs. Cell Stem Cell *3*, 301–313.

Crisan, M., Corselli, M., Chen, W.C., and Péault, B. (2012). Perivascular cells for regenerative medicine. J. Cell. Mol. Med. *16*, 2851–2860.

Dar, A., and Itskovitz-Eldor, J. (2013). Therapeutic potential of perivascular cells from human pluripotent stem cells. J. Tissue Eng. Regen. Med. Published online January 31, 2013. http://dx.doi.org/10.1002/term.1698.

Dar, A., Domev, H., Ben-Yosef, O., Tzukerman, M., Zeevi-Levin, N., Novak, A., Germanguz, I., Amit, M., and Itskovitz-Eldor, J. (2012). Multipotent vasculogenic pericytes from human pluripotent stem cells promote recovery of murine ischemic limb. Circulation *125*, 87–99.

Deguchi, S., Ohashi, T., and Sato, M. (2006). Tensile properties of single stress fibers isolated from cultured vascular smooth muscle cells. J. Biomech. *39*, 2603–2610.

Díaz-Flores, L., Gutiérrez, R., Madrid, J.F., Varela, H., Valladares, F., Acosta, E., Martín-Vasallo, P., and Díaz-Flores, L., Jr. (2009). Pericytes. Morphofunction, interactions and pathology in a quiescent and activated mesenchymal cell niche. Histol. Histopathol. *24*, 909–969.

Drukker, M., Tang, C., Ardehali, R., Rinkevich, Y., Seita, J., Lee, A.S., Mosley, A.R., Weissman, I.L., and Soen, Y. (2012). Isolation of primitive endoderm, mesoderm, vascular endothelial and trophoblast progenitors from human pluripotent stem cells. Nat. Biotechnol. *30*, 531–542.

Eble, J.A., and Niland, S. (2009). The extracellular matrix of blood vessels. Curr. Pharm. Des. *15*, 1385–1400.

Elia, L., Quintavalle, M., Zhang, J., Contu, R., Cossu, L., Latronico, M.V.G., Peterson, K.L., Indolfi, C., Catalucci, D., Chen, J., et al. (2009). The knockout of miR-143 and -145 alters smooth muscle cell maintenance and vascular homeostasis in mice: correlates with human disease. Cell Death Differ. *16*, 1590–1598.

Evseenko, D., Zhu, Y., Schenke-Layland, K., Kuo, J., Latour, B., Ge, S., Scholes, J., Dravid, G., Li, X., MacLellan, W.R., and Crooks, G.M. (2010). Mapping the first stages of mesoderm commitment during differentiation of human embryonic stem cells. Proc. Natl. Acad. Sci. USA *107*, 13742–13747.

Ferreira, L.S., Gerecht, S., Shieh, H.F., Watson, N., Rupnick, M.A., Dallabrida, S.M., Vunjak-Novakovic, G., and Langer, R. (2007). Vascular progenitor cells isolated from human embryonic stem cells give rise to endothelial and smooth muscle like cells and form vascular networks in vivo. Circ. Res. *101*, 286–294.

Glukhova, M.A., Frid, M.G., Shekhonin, B.V., Vasilevskaya, T.D., Grunwald, J., Saginati, M., and Koteliansky, V.E. (1989). Expression of extra domain A fibronectin sequence in vascular smooth muscle cells is phenotype dependent. J. Cell Biol. *109*, 357–366.

Görlach, A., Klappa, P., and Kietzmann, D.T. (2006). The endoplasmic reticulum: folding, calcium homeostasis, signaling, and redox control. Antioxid. Redox Signal *8*, 1391–1418.

Hedin, U., and Thyberg, J. (1987). Plasma fibronectin promotes modulation of arterial smooth-muscle cells from contractile to synthetic phenotype. Differentiation *33*, 239–246.

Karnik, S.K., Brooke, B.S., Bayes-Genis, A., Sorensen, L., Wythe, J.D., Schwartz, R.S., Keating, M.T., and Li, D.Y. (2003). A critical role for elastin signaling in vascular morphogenesis and disease. Development *130*, 411–423.

Kumar, V.A., Brewster, L.P., Caves, J.M., and Chaikof, E.L. (2011). Tissue engineering of blood vessels: functional requirements, progress, and future challenges. Cardiovasc. Eng. Technol. *2*, 137–148.

Kusuma, S., and Gerecht, S. (2013). Recent progress in the use of induced pluripotent stem cells in vascular regeneration. Expert Rev. Cardiovasc. Ther. *11*, 661–663.

Kusuma, S., Shen, Y.-I., Hanjaya-Putra, D., Mali, P., Cheng, L., and Gerecht, S. (2013). Self-organized vascular networks from human pluripotent stem cells in a synthetic matrix. Proc. Natl. Acad. Sci. USA *110*, 12601–12606.

Li, A.-F., Sato, T., Haimovici, R., Okamoto, T., and Roy, S. (2003). High glucose alters connexin 43 expression and gap junction intercellular communication activity in retinal pericytes. Invest. Ophthalmol. Vis. Sci. *44*, 5376–5382.

Liang, B., Wang, S., Wang, Q., Zhang, W., Viollet, B., Zhu, Y., and Zou, M.-H. (2013). Aberrant endoplasmic reticulum stress in vascular smooth muscle increases vascular contractility and blood pressure in mice deficient of AMP-activated protein kinase-α2 in vivo. Arterioscler. Thromb. Vasc. Biol. *33*, 595–604.

Louis, S.F., and Zahradka, P. (2010). Vascular smooth muscle cell motility: from migration to invasion. Exp. Clin. Cardiol. *15*, e75–e85.

Majesky, M.W. (2007). Developmental basis of vascular smooth muscle diversity. Arterioscler. Thromb. Vasc. Biol. *27*, 1248–1258.

Murfee, W.L., Skalak, T.C., and Peirce, S.M. (2005). Differential arterial/venous expression of NG2 proteoglycan in perivascular cells along microvessels: identifying a venule-specific phenotype. Microcirculation *12*, 151–160.

Newby, A.C. (2006). Matrix metalloproteinases regulate migration, proliferation, and death of vascular smooth muscle cells by degrading matrix and non-matrix substrates. Cardiovasc. Res. *69*, 614–624.

Niland, J.A.E.S. (2009). The extracellular matrix of blood vessels. Curr. Pharm. Des. *15*, 1385–1400.

Orlova, V.V., Drabsch, Y., Freund, C., Petrus-Reurer, S., van den Hil, F.E., Muenthaisong, S., ten Dijke, P., and Mummery, C.L. (2014). Functionality of endothelial cells and pericytes from human pluripotent stem cells demonstrated in cultured vascular plexus

and zebrafish xenografts. Arterioscler. Thromb. Vasc. Biol. *34*, 177–186.

Ozerdem, U., Grako, K.A., Dahlin-Huppe, K., Monosov, E., and Stallcup, W.B. (2001). NG2 proteoglycan is expressed exclusively by mural cells during vascular morphogenesis. Dev. Dyn. *222*, 218–227.

Patel, A., Fine, B., Sandig, M., and Mequanint, K. (2006). Elastin biosynthesis: the missing link in tissue-engineered blood vessels. Cardiovasc. Res. *71*, 40–49.

Raffetto, J.D., and Khalil, R.A. (2008). Matrix metalloproteinases and their inhibitors in vascular remodeling and vascular disease. Biochem. Pharmacol. *75*, 346–359.

Rekhter, M.D. (1999). Collagen synthesis in atherosclerosis: too much and not enough. Cardiovasc. Res. *41*, 376–384.

Rzucidlo, E.M., Martin, K.A., and Powell, R.J. (2007). Regulation of vascular smooth muscle cell differentiation. J. Vasc. Surg. *45* (*Suppl A*), A25–A32.

Schönthal, A.H. (2012). Endoplasmic reticulum stress: its role in disease and novel prospects for therapy. Scientifica (Cairo) *2012*, 857516.

Shekhonin, B.V., Domogatsky, S.P., Muzykantov, V.R., Idelson, G.L., and Rukosuev, V.S. (1985). Distribution of type I, III, IV and V collagen in normal and atherosclerotic human arterial wall: immunomorphological characteristics. Coll. Relat. Res. *5*, 355–368.

Shekhonin, B.V., Domogatsky, S.P., Idelson, G.L., Koteliansky, V.E., and Rukosuev, V.S. (1987). Relative distribution of fibronectin and type I, III, IV, V collagens in normal and atherosclerotic intima of human arteries. Atherosclerosis *67*, 9–16.

Sprague, A.H., and Khalil, R.A. (2009). Inflammatory cytokines in vascular dysfunction and vascular disease. Biochem. Pharmacol. *78*, 539–552.

Tabas, I. (2010). The role of endoplasmic reticulum stress in the progression of atherosclerosis. Circ. Res. *107*, 839–850.

Tang, Z., Wang, A., Yuan, F., Yan, Z., Liu, B., Chu, J.S., Helms, J.A., and Li, S. (2012). Differentiation of multipotent vascular stem cells contributes to vascular diseases. Nat. Commun. *3*, 875.

Thyberg, J., Blomgren, K., Roy, J., Tran, P.K., and Hedin, U. (1997). Phenotypic modulation of smooth muscle cells after arterial injury is associated with changes in the distribution of laminin and fibronectin. J. Histochem. Cytochem. *45*, 837–846.

Urbán, Z., Riazi, S., Seidl, T.L., Katahira, J., Smoot, L.B., Chitayat, D., Boyd, C.D., and Hinek, A. (2002). Connection between elastin haploinsufficiency and increased cell proliferation in patients with supravalvular aortic stenosis and Williams-Beuren syndrome. Am. J. Hum. Genet. *71*, 30–44.

Virgintino, D., Girolamo, F., Errede, M., Capobianco, C., Robertson, D., Stallcup, W.B., Perris, R., and Roncali, L. (2007). An intimate interplay between precocious, migrating pericytes and endothelial cells governs human fetal brain angiogenesis. Angiogenesis *10*, 35–45.

Vo, E., Hanjaya-Putra, D., Zha, Y., Kusuma, S., and Gerecht, S. (2010). Smooth-muscle-like cells derived from human embryonic stem cells support and augment cord-like structures in vitro. Stem Cell Rev. *6*, 237–247.

Vodyanik, M.A., Yu, J., Zhang, X., Tian, S., Stewart, R., Thomson, J.A., and Slukvin, I.I. (2010). A mesoderm-derived precursor for mesenchymal stem and endothelial cells. Cell Stem Cell *7*, 718–729.

Wanjare, M., Kuo, F., and Gerecht, S. (2013a). Derivation and maturation of synthetic and contractile vascular smooth muscle cells from human pluripotent stem cells. Cardiovasc. Res. *97*, 321–330.

Wanjare, M., Kusuma, S., and Gerecht, S. (2013b). Perivascular cells in blood vessel regeneration. Biotechnol. J. *8*, 434–447.

Wei, S., Gao, X., Du, J., Su, J., and Xu, Z. (2011). Angiogenin enhances cell migration by regulating stress fiber assembly and focal adhesion dynamics. PLoS ONE *6*, e28797.

Stem Cell Reports, Volume *2*

Supplemental Information

Defining Differences among Perivascular Cells Derived from Human Pluripotent Stem Cells

Maureen Wanjare, Sravanti Kusuma, and Sharon Gerecht

Supplementary Figures and Figure Legends

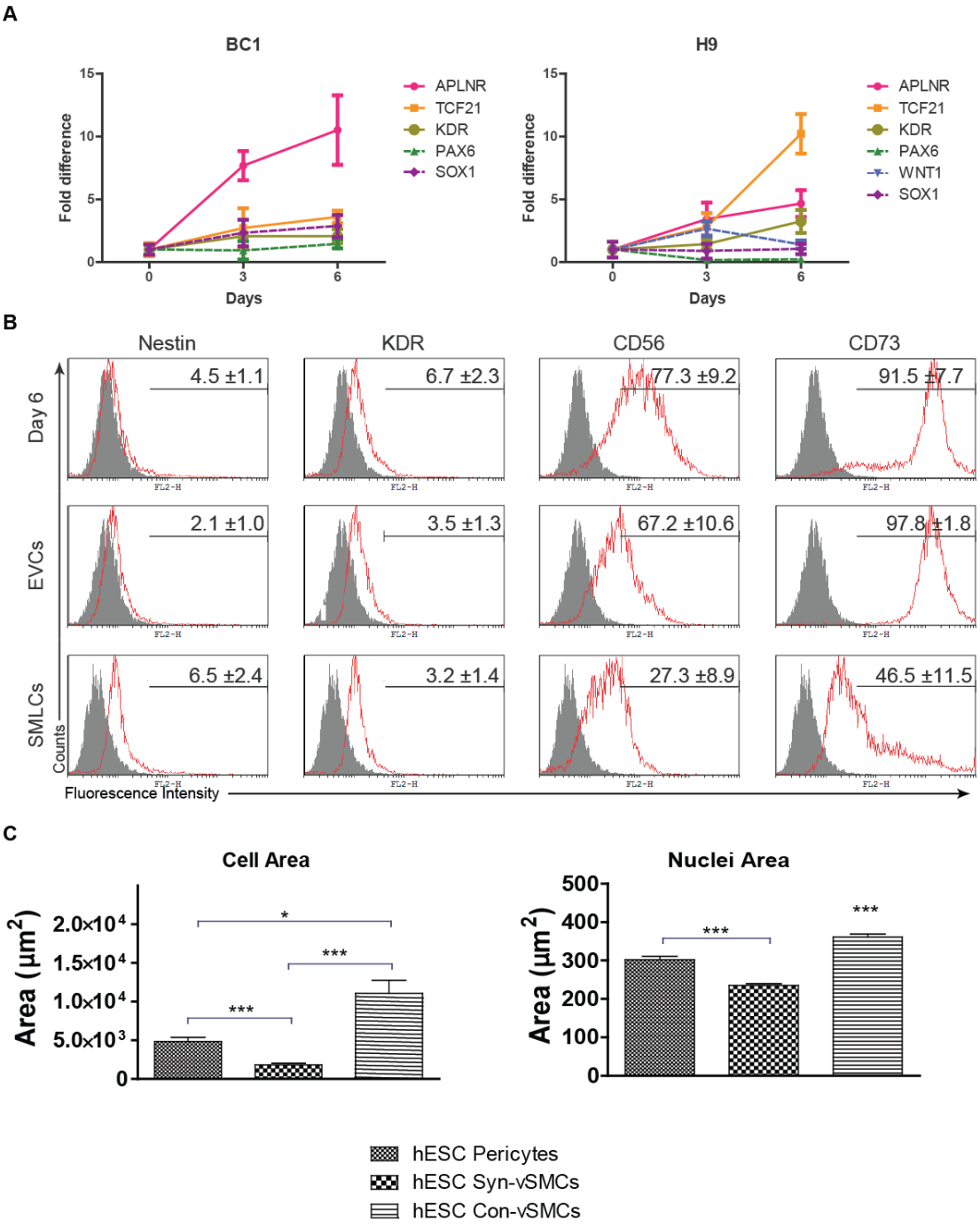

Figure S1. Marker assessment of perivascular derivatives related to Figure 1. (A) Quantitative real time RT-PCR analysis of mesoderm (in solid lines) and neural crest (in dashed lines) genes at days 0, 3 and 6 along differentiation for BC1 and H9 (n=3 biological replicates). **(B-C)** H9 differentiating cells analyzed for **(B)** marker expression by flow cytometry analysis of day 6 differentiating cells, EVCs, and SMLCs (isotype control in gray) and **(C)** perivascular cell and nuclei area. Results shown are representative of three independent experiments. All graphical data are reported as mean ±SEM.

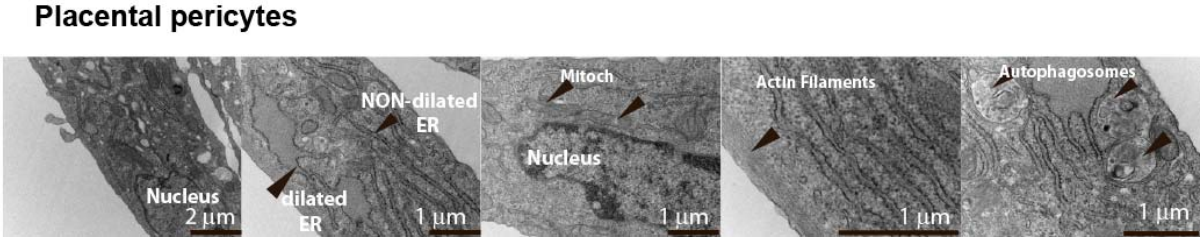

Figure S2. Control pericytes, related to Figure 2. Placenta pericytes were analyzed for sub-cellular organelle organization using TEM.

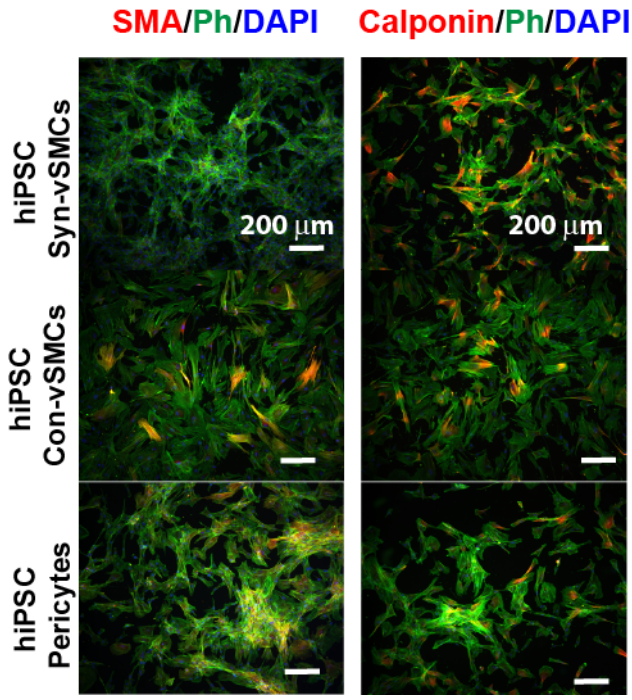

Figure S3. Differences in stress fiber and contractile marker expression, related to Figure 3. Perivascular derivatives were assessed by immunofluorescence for αSMA and calponin (in red; phalloidin in green; nuclei in blue). Figures shown are low magnification representative images of Fig. 3A.

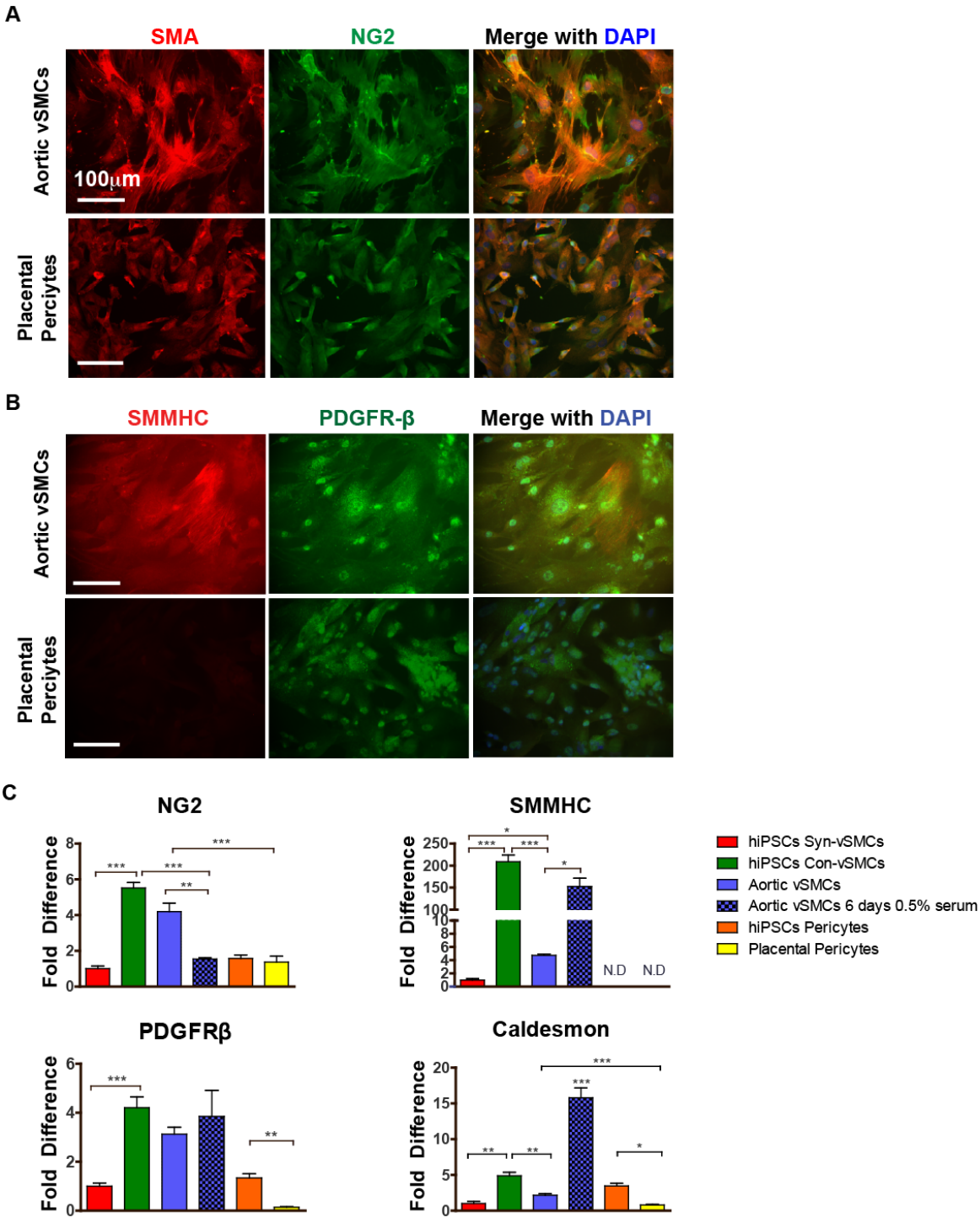

Figure S4. Perivascular marker expression in control cells related to Figure 3. Organization of **(A)** SMA (red) and NG2 (green; nuclei in blue) and **(B)** SMMHC (red) and PDGFRβ (green; nuclei in blue) in aortic vSMCs and placenta pericytes. **(C)** Expression of NG2, SMMHC, PDGFRβ and caldesmon in the different cell types compared to aortic vSMCs starved in low serum using quantitative real time RT-PCR. Results shown from three independent experiments; each RT-PCR sample was run with three technical replicates. All graphical data are reported as mean ±SEM. *P<0.05; **P<0.01; ***P<0.001.

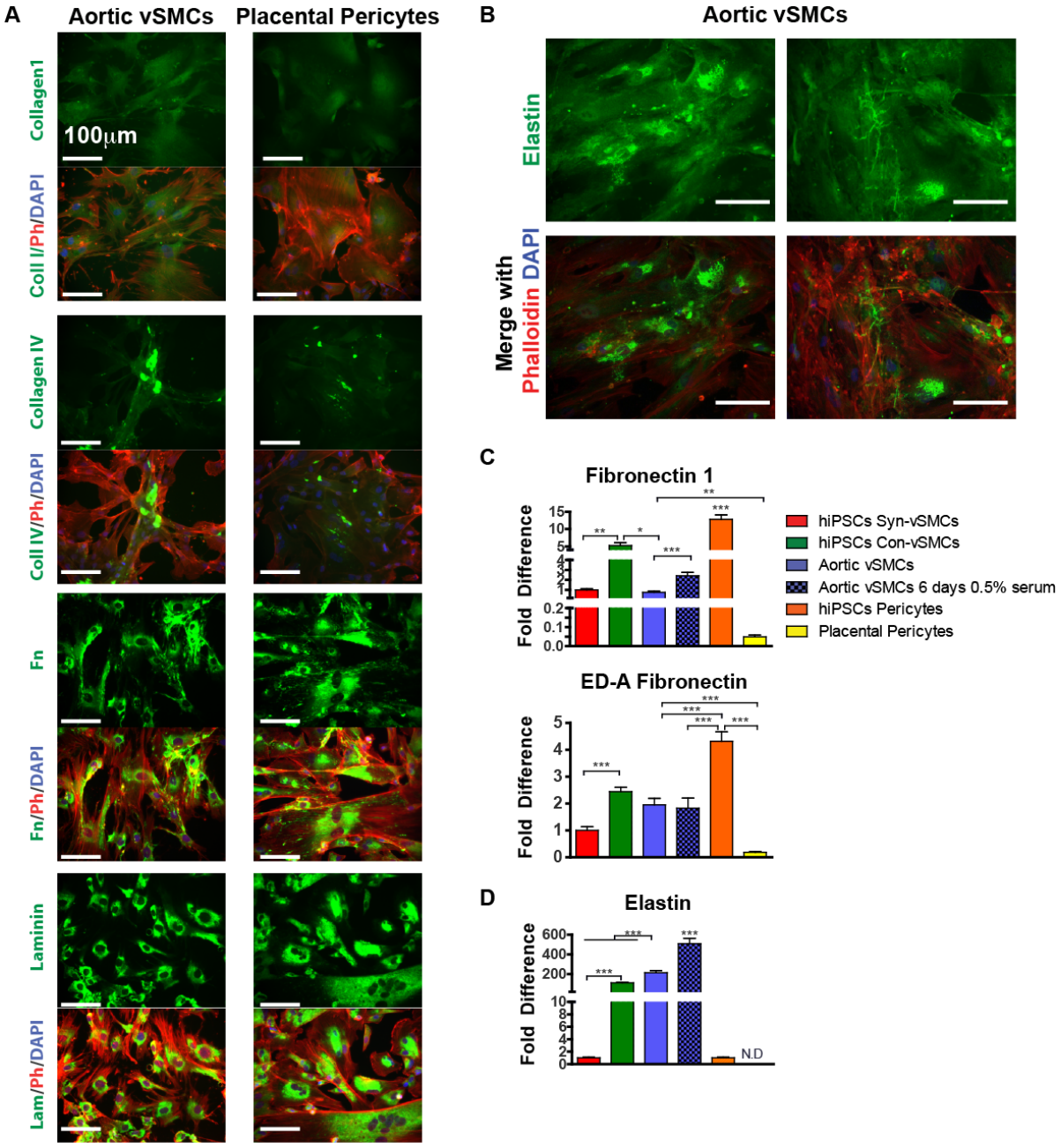

Figure S5. ECM in control cells related to Figure 4. (A) Deposition of the ECM proteins collagen I, collagen IV, fibronectin, and laminin (all in green; phalloidin in red; nuclei in blue.) in placenta pericytes and aortic vSMCs. **(B)** Elastin organization in aortic vSMCs (in green; phalloidin in red; nuclei in blue) showing interacellular (left column) and extracellular (right column) deposition. **(C-D)** Expression of fibronectin, ED-A fibronectin and elastin, in the different cell types (compared to aortic vSMCs starved in low serum) using quantitative real time RT-PCR. Results shown from three independent experiments; each RT-PCR sample was run with three technical replicates. All graphical data are reported as mean ±SEM. *P<0.05; **P<0.01; ***P<0.001.

Supplemental Experimental Procedures

Cell Culture

All cells were cultured in humidified incubators, with atmospheres at 37°C and 5% CO_2.

Human PSCs. hiPSC line BC1 (Cheng et al., 2012; Chou et al., 2011) kindly provided by Dr. Cheng, SOM JHU and Human ESC line H9 (passages 15 to 40; WiCell Research Institute, Madison, WI) were grown on inactivated mouse embryonic fibroblast feeder layers (GlobalStem, Rockville, MD) in growth medium composed of 80 percent ES-DMEM/F12 (GlobalStem), 20 percent knockout serum replacement (Invitrogen, Carlsbad, CA), and 4 ng/ml basic fibroblast growth factor (bFGF; Invitrogen) for hEScs of 10ng/ml bFGF for hiPSCs, as previously reported (Wanjare et al., 2013). Human iPSCs were passaged every four to six days using 1 mg/ml of type IV collagenase (Invitrogen). Media were changed daily.

Human v-SMCs. The control cell type used was human aorta v-SMCs (passages 4-7; ATCC, Manassas, VA). The cells were cultured in the specified ATCC complete SMC growth medium, composed of Kaighn's Modification of Ham's F-12 Medium (F-12K Medium; ATCC), 10% or 0.5% fetal bovine serum (FBS; Hyclone), 0.01 mg/ml transferrin (Sigma-Aldrich, St. Louis, MO), 0.01 mg/ml insulin (Sigma), 10 mM HEPES buffer (Sigma), 10 mM 2-(Tris(hydroxymethyl)methylamino)ethane-1-sulphonic acid (TES)(Sigma), 0.05 mg/ml ascorbic acid (Sigma), 10 ng/mL sodium selenite (Sigma), and 0.03 mg/ml Endothelial Cell Growth Supplement (Sigma). Human v-SMCs were passaged every three to four days using 0.25 percent trypsin (Invitrogen). Media was changed every two to three days.

Human pericytes. The control cell type used was human placental pericytes (passages 3-5; Promocell). The cells were cultured in the specified Pericyte Growth Media (Promocell) and were passaged every three to four days using a detatchment kit (Promocell).

vSMC differentiation protocol

vSMCs were derived as previously described (Wanjare et al., 2012). Briefly, hPSCs were collected through digestion with TrypLE (Invitrogen) and were seeded at a concentration of $5x10^4$ cells/cm^2 onto plates previously coated with collagen type IV (R&D Systems, Minneapolis, MN). The hPSCs were cultured for six days in a differentiation medium, composed of alpha-MEM (Invitrogen), 10% FBS (Hyclone), and 0.1 mM β-mercaptoethanol (Invitrogen). Media were changed daily. On day six, the differentiated cells were collected through digestion with TrypLE (Invitrogen), separated with a 40-μm mesh strainer, and seeded at a concentration of $1.25x10^4$ cells/cm^2 on collagen-type-IV-coated plates. The differentiating hPSCs were then cultured in differentiation medium; with the addition of 10 ng/ml PDGF-BB (R&D Systems) and 1 ng/ml TGF-β1 (R&D Systems) for additional 6 days (total of 12 days) for SMLCs. Media was changed every second day. Serum starved cells were passaged every 6-8 days with Tryple, using alpha-MEM (Invitrogen), 10% FBS (Hyclone), and 0.1 mM β-mercaptoethanol (Invitrogen) to neutralize Tryple but then seeded with 0.5% serum media.

Pericyte differentiation protocol

Pericytes were differentiated as previously described (Kusuma et al., 2013; Orlidge and D'Amore, 1987). Briefly, hPSCs were differentiated as described for vSMC differentiation above for the first 6 days. On day 6, cells were re-seeded at a concentration of $1.25x10^4$ cells/cm^2 on collagen-type-IV-coated plates in endothelial cell growth media (ECGM) (PromoCell) supplemented with 2% FBS, 50ng/ml vascular endothelial growth factor (VEGF), and 10μM SB431542 (Tocris) for 6 days. Media was changed every other day. On day 12, derived EVCs

were collected through digestion with TrypLE and replated on tissue culture-treated six-well plates in medium composed of DMEM and 10% FBS. After 2–3 h, unattached cells were removed, and the medium was replaced. Cells were cultured for 6 d, with the medium changed every other day.

Flow cytometry

Flow cytometry was performed as previously described (Kusuma et al., 2012). Briefly, cells were incubated with PE-conjugated antigen specific antibodies for markers outlined in the text including KDR-PE (1:10; BD), Nestin-PE (1:10; BD), CD56-PE (1:10; BD); SMMHC-PE (1:10; MYH11; Santa Cruz). To detect SMMHC -PE, cells were fixed with 3.7% formaldehyde for 10 minutes, washed, incubated with 0.1% Triton X for 10 minutes, washed, and finally incubated with SMMHC -PE for 45 minutes. All analyses were done using corresponding isotype controls. Forward-side scatter plots were used to exclude dead cells. User guide instructions were followed to complete the flow cytometry analysis via Cyflogic v1.2.

Immunofluorescence

Cells were prepared for immunofluorescence as previously described (Kusuma et al., 2012; Wanjare et al., 2012). Cells were fixed using 3.7% formaldehyde fixative for 15 minutes, washed with phosphate buffered saline (PBS), blocked with 1% bovine serum albumin (BSA) in PBS for 1 hour minimum, permeabilized with a solution of 0.1% Triton-X (Sigma) for ten minutes, washed with PBS, and incubated for one hour with anti-human SMA (1:200; Dako, Glostrup, Denmark), anti-human NG2 (1:100; Santa Cruz), anti-human PDGFRβ (1:100, Santa Cruz), and anti-human SMMHC (3:100; Dako). For ECM staining, cells were incubated with anti-human fibronectin (1:200; Sigma), anti-human collagen1 (1:200; Abcam), anti-human collagen IV (1:100; Abcam), anti-human laminin (1:200; Abcam) or anti-human elastin (3:100 Abcam) for one hour. Cells were rinsed twice with PBS and incubated with Alexa 546

conjugated phalloidin (1:100; Molecular Probes, Eugene, OR) or anti-mouse IgG Cy3 conjugate (1:50; Sigma), anti-mouse FITC (1:50; Sigma), or anti-rabbit IgG Alexa Fluor 488 conjugate (1:1000; Molecular Probes, Eugene, OR) for one hour, rinsed with PBS, and incubated with DAPI (1:1000; Roche Diagnostics) for ten minutes. Coverslips were rinsed once more with PBS and mounted with fluorescent mounting medium (Dako). The immunolabeled cells were examined using fluorescence microscopy (Olympus BX60; Olympus, Center Valley, PA) and confocal microscopy (LSM 510 Meta; Carl Zeiss).

Cellular characterizations

The nuclei size of cells was quantified in ImageJ by thresholding fluorescence intensities of DAPI. The cellular area was quantified by thresholding the fluorescent intensities of the membrane dyes FM464. The percentage of replicating cells was quantified in ImageJ by taking the ratio between the number of Ki67 fluorescent positive cells and the fluorescent DAPI. At least three fields of view were imaged at 10x for each sample.

Transmission electron microscopy (TEM)

Differentiated cells, placental pericytes, and aortic vSMCs were prepared for TEM analysis as described previously (Hanjaya-Putra et al., 2011). Serial sections were cut, mounted onto copper grids, and viewed using a Phillips EM 410 TEM (FEI, Hillsboro, OR,USA). Images were captured using a SIS Megaview III CCD (Lakewood,CO, USA).

Stress fiber quantification

The number of stress fibers per cell was quantified using line intensity profiles of cells in ImageJ (Wei et al., 2011). Stress fibers were labeled with fluorescent Alexa-488 phalloidin and imaged at 20x and 40x. A line intensity profile across a single cell was generated with each peak representing a single stress fiber.

Real-time quantitative RT-PCR

Two-step RT-PCR was performed on differentiated hPSCs at various time points as we previously described (Wanjare et al., 2012). Total RNA was extracted by using TRIzol (Gibco, Invitrogen), as per the manufacturer's instructions. All samples were verified as free of DNA contamination. The concentration of total RNA was quantified using an ultraviolet spectrophotometer. RNA (1 µg per sample) was transcribed using the reverse transcriptase M-MLV (Promega Co., Madison, WI) and oligo(dT) primers (Promega), as per the manufacturer's instructions. The specific assay used was the TaqMan Universal PCR Master Mix and Gene Expression Assay (Applied Biosystems, Foster City, CA) for *ACTA2*, *CNN1*, *CSPG4*, *PDGFRB*, *MYH11*, *COLA1, COL4A1, LAMC1, ELN , MMP14, CALD1, ALPNR, TCF21, KDR, PAX6, WNT1, SOX1, ACTB*, and *GAPDH*, as per the manufacturer's instructions. Assays on Demand Kits (Applied Biosystems, Foster City, CA, USA) was used for *FN1* (Hs01549958) and the customized (Applied Biosystems, Foster City, CA, USA) ED-A spanning exons sequence primer was: Forward 5'-CCAGTGCACAGCTATTCCTG-3' and Reverse 5'-ACAACCACGGATGAGCTG-3' (Forte et al., 2013; van der Straaten et al., 2004).

The Taqman PCR step was performed with an Applied Biosystems StepOne Real-Time PCR System (Applied Biosystems), in accordance with the manufacturer's instructions. The relative expressions of the genes were normalized to the amount of *ACTB* or *GAPDH* in the same cDNA by using the standard curve method provided by the manufacturer. For each primer set, the comparative computerized tomography method (Applied Biosystems) was used to calculate the amplification differences between the different samples. The values for the experiments were averaged and graphed with standard deviations.

Zymography

Zymography was performed to determine MMP activities as previously (Hanjaya-Putra et al., 2012). MMP1 was detected using SDS-Page casein zymography while both MMP2 and MMP9 were detected using SDS-Page gelatin zymography. Cells were cultured in serum free media for 72 hours. We collected the media of each sample and loaded the media of the samples per well into either a casein gel (BioRad) or gelatin gel (BioRad). Quantification of protein was done using the Bradford Assay. After electrophoresis, the gels were renatured by washing in renaturation buffer (Invitrogen) and incubated at 37˚C in denaturation buffer (Invitrogen) for 24h. The proteins were fixed in 50% methanol and 10% acetic acid for 30 min and then stained in 0.02% commasie blue (Sigma). Gels were destained in 20%methanol and 10% acetic acid and were visualized using the ChemiDoc XRS+ System (BioRad). Images were acquired using BioRad Quantity One software.

Mesenchymal differentiation (adipogenic and osteogenic)

We followed our previously published protocol for mesenchymal differentiations (Kusuma et al., 2013). For adipogenic differentiation (Pittenger et al., 1999), we cultured derived pericytes at 10,000cells/cm^2 in media comprised of DMEM, 10% FBS, 1% Penicillin/Streptomycin, 200μM Indomethacin, 500 μM 3-Isobutyl-1-methyl xanthine (IBMX), and 5 μg/ml Insulin (all from Sigma) for 4 weeks. To assess adipogenic potential, cells were fixed with 3.7% formaldehyde, then dehydrated with 60% isopropanol for 5 minutes. Cells were incubated with Oil Red O (Sigma) at 1.8 mg/ml in 60/40 isopropanol/DI H_2O, for 10 minutes and imaged using an inverted light microscope (Olympus).

For osteogenic differentiation (Grayson et al., 2010), we cultured derived pericytes at 5,000cells/cm^2 in media comprised of low glucose DMEM, 10% FBS, 1% Penicillin/Streptomycin, 10mM β-glycerophosphate, 100nM dexamethasone, and 50 μM ascorbic acid (all from Sigma) for 2 weeks. Media were prepared fresh weekly. To assess

osteogenic potential, samples were fixed with 3.7% formaldehyde, and washed with DI H_2O. Samples were incubated with Alizarin Red S (40mM in DI H_2O, pH ~4.2; Sigma) for 10-20 minutes.

Subcutaneous Matrigel implantation

hiPSC-derived perivascular cells were trypsinized, collected and stained with PKH26 (Sigma-Aldrich) membrane dye. We encapsulated a total of 0.5×10^6 PSC-vSMCs in reduced growth factor Matrigel (BD Biosciences) and 20 µL of EGM-2 media (endothelial growth media). The Matrigel, which contained 250 ng/mL of bFGF (R&D Systems), was loaded, along with the cell mixture, into a 1 mL syringe with a 22-gauge needle and injected subcutaneously into each side of the dorsal region of six- to eight-week-old nude mice. On day 7, we injected isolectin GS-IB4, an Alexa Fluor(R) 488 conjugate glycoprotein isolated from the Griffonia simplicifolia African legume (Invitrogen) through the tail veins of the mice. After 20 minutes, we euthanized the mice by CO2 asphyxiation and harvested the Matrigel plugs, which were fixed in 3.7 percent formaldehyde (Sigma-Aldrich) for one hour, and incubated with DAPI (1:1000; Roche Diagnostics) for ten minutes. A sequence of z-stack images was obtained using confocal microscopy (LSM 510 Meta, Carl Zeiss, Inc.). The Johns Hopkins University Institutional Animal Care and Use Committee approved all animal protocols.

Wound healing assay

Migration of the derived hiPSC perivascular cells was assessed using a wound healing assay (Rodriguez et al., 2005). Cells were cultured to a confluent monolayer in a 6 well plate. Cell monolayers were wounded by scratching a strip of cells with a 200uL pipette tip. After the detached cells were removed and the cells were washed, fresh medium containing 0.5% serum was added. Cells were incubated in a humidified incubator coupled to a microscope, which took

a series of images of the migration of the cells into the gap every 10 min for 24 h. Migration trajectories and speed was calculated using the MTrackJ plugin of ImageJ (NIH).

Invasion toward ECs

A downward invasion toward ECs assay was used to assess invasion of perivascular cells. Human umbilical vein endothelial cells (HUVECs) were seeded on 16 well detachable wells (Fisher). After 24 h, 150 ul of collagen gel was added on top of the HUVECs. Stock solution was used to prepare collagen gels at a density of 2.5 mg/ml. Gel formation was achieved by simultaneously decreasing the solution's pH and increasing the temperature to 37°C. To prepare 150 ul of collagen gels, we mixed 66.1 ul M199 1X with 6.44 ul M199 10x. To this, we added 57.8 ul collagen type I. After the addition of approximately 2 ul 1M NaOH, the solution was thoroughly mixed and added to the HUVEC monolayer. The gel was allowed to polymerize for 1h at 37°C in a CO_2 incubator. Upon polymerization, hiPSC perivascular cells were cultured on top of the gels to allow downward invasion. After 48h the gels were fixed using 3% gluteraldehyde for 30min, stained with 0.1% toluidine blue dye for 15 min, and washed with distilled water. Cross-sections of the gels were imaged using Accuscope. Quantification of invasion distance into the collagen gel was performed using ImageJ.

Functional contraction studies

Contraction studies in response to pharmacological drugs were done, as previously described (Vo et al., 2010; Wanjare et al., 2012). Briefly, perivascular cell derivatives were cultured, washed, and contraction was induced by incubating with 10^{-5} M carbachol (Calbiochem, Darmstadt, Germany) in DMEM medium (Invitrogen) for 30 minutes. The perivascular cell derivatives were visualized using cytoplasm-viable fluorescence dye, calceine. A series of time-lapse images were taken using a microscope with a 10X objective lens (Axiovert; Carl Zeiss). The cell contraction percentage was calculated by the difference in area

covered by the cells before (at time zero) and after contraction (at time 30 minutes). Area analysis was performed with Adobe Photoshop CS5 (Adobe Systems Inc., Mountain View, CA). Each set of images was analyzed three times. The magic wand and measurement tools were used to calculate the area of the image not covered in cells, which was then subtracted from the total area of the image. This method improves upon our previously established procedure (Vo et al., 2010) by eliminating the need for image compression and by increasing the consistency of cell selection within each set of images.

Statistical analysis

Real-time RT-PCR, functionality assays, flow cytometry and image analyses were performed in at least triplicate biological samples. Real-time RT-PCR analyses were also performed with triplicate readings. Statistical analyses were performed with GraphPad Prism 4.02 (GraphPad Software Inc., La Jolla, CA). Unpaired two-tailed t-tests and one-way ANOVA analysis and Bonferonni post tests were performed where appropriate using GraphPad Prism 4.02 (GraphPad Software Inc., La Jolla, CA). Significance levels were set at $*p<0.05$, $**p<0.01$, and $***p<0.001$. All graphical data are reported as mean ±SEM.

Supplemental References

Cheng, L., Hansen, Nancy F., Zhao, L., Du, Y., Zou, C., Donovan, Frank X., Chou, B.-K., Zhou, G., Li, S., Dowey, Sarah N.*, et al.* (2012). Low Incidence of DNA Sequence Variation in Human Induced Pluripotent Stem Cells Generated by Nonintegrating Plasmid Expression. Cell Stem Cell *10*, 337-344.

Chou, B.K., Mali, P., Huang, X., Ye, Z., Dowey, S.N., Resar, L.M.S., Zou, C., Zhang, Y.A., Tong, J., and Cheng, L. (2011). Efficient human iPS cell derivation by a non-integrating plasmid from blood cells with unique epigenetic and gene expression signatures. Cell Research *21*, 518-529.

Forte, A., Della Corte, A., Grossi, M., Bancone, C., Provenzano, R., Finicelli, M., De Feo, M., De Santo, L.S., Nappi, G., Cotrufo, M.*, et al.* (2013). Early cell changes and TGFβ pathway alterations in the aortopathy associated with bicuspid aortic valve stenosis. Clinical Science *124*, 97-108.

Grayson, W.L., Frohlich, M., Yeager, K., Bhumiratana, S., Chan, M.E., Cannizzaro, C., Wan, L.Q., Liu, X.S., Guo, X.E., and Vunjak-Novakovic, G. (2010). Engineering anatomically shaped human bone grafts. Proceedings of the National Academy of Sciences of the United States of America *107*, 3299-3304.

Hanjaya-Putra, D., Bose, V., Shen, Y.-I., Yee, J., Khetan, S., Fox-Talbot, K., Steenbergen, C., Burdick, J.A., and Gerecht, S. (2011). Controlled activation of morphogenesis to generate a functional human microvasculature in a synthetic matrix. Blood *118*, 804-815.

Hanjaya-Putra, D., Wong, K.T., Hirotsu, K., Khetan, S., Burdick, J.A., and Gerecht, S. (2012). Spatial control of cell-mediated degradation to regulate vasculogenesis and angiogenesis in hyaluronan hydrogels. Biomaterials *33*, 6123-6131.

Kusuma, S., Shen, Y.-I., Hanjaya-Putra, D., Mali, P., Cheng, L., and Gerecht, S. (2013). Self-organized vascular networks from human pluripotent stem cells in a synthetic matrix. Proceedings of the National Academy of Sciences *110*, 12601-12606..

Kusuma, S., Zhao, S., and Gerecht, S. (2012). The extracellular matrix is a novel attribute of endothelial progenitors and of hypoxic mature endothelial cells. FASEB Journal *26*, 4925-4936.

Orlidge, A., and D'Amore, P.A. (1987). Inhibition of capillary endothelial cell growth by pericytes and smooth muscle cells. The Journal of Cell Biology *105*, 1455-1462.

Pittenger, M.F., Mackay, A.M., Beck, S.C., Jaiswal, R.K., Douglas, R., Mosca, J.D., Moorman, M.A., Simonetti, D.W., Craig, S., and Marshak, D.R. (1999). Multilineage potential of adult human mesenchymal stem cells. Science *284*, 143-147.

Rodriguez, L.G., Wu, X., and Guan, J.-L. (2005). Wound-healing assay. In Cell Migration (Springer), pp. 23-29.

van der Straaten, H.M., Canninga-van Dijk, M.R., Verdonck, L.F., Castigliego, D., Borst, H., Aten, J., and Fijnheer, R. (2004). Extra-Domain-A Fibronectin: A New Marker of Fibrosis in Cutaneous Graft-Versus-Host Disease. J Investig Dermatol *123*, 1057-1062.

Vo, E., Hanjaya-Putra, D., Zha, Y., Kusuma, S., and Gerecht, S. (2010). Smooth-muscle-like cells derived from human embryonic stem cells support and augment cord-like structures in vitro. Stem Cell Rev *6*, 237-247.

Wanjare, M., Kuo, F., and Gerecht, S. (2012). Derivation and maturation of synthetic and contractile vascular smooth muscle cells from human pluripotent stem cells. Cardiovascular Research *97*, 321-330.

Wanjare, M., Kuo, F., and Gerecht, S. (2013). Derivation and maturation of synthetic and contractile vascular smooth muscle cells from human pluripotent stem cells. Cardiovascular Research *97*, 321-330.

Wei, S., Gao, X., Du, J., Su, J., and Xu, Z. (2011). Angiogenin Enhances Cell Migration by Regulating Stress Fiber Assembly and Focal Adhesion Dynamics. PLoS ONE *6*, e28797.